

---

# Computing Exact Shapley Values in Polynomial Time for Product-Kernel Methods

---

**Majid Mohammadi**

CISPA Helmholtz Center for Information Security, Germany  
Vrije Universiteit Amsterdam, The Netherlands

**Siu Lun Chau**

College of Computing & Data Science  
Nanyang Technological University  
Singapore

**Krikamol Muandet**

Rational Intelligence Lab  
CISPA Helmholtz Center for Information Security  
Germany

## Abstract

Kernel methods are widely used in machine learning due to their flexibility and expressive power. However, their black-box nature poses significant challenges to interpretability, limiting their adoption in high-stakes applications. Shapley value-based feature attribution techniques, such as SHAP and kernel-specific variants like RKHS-SHAP, offer a promising path toward explainability. Yet, computing exact Shapley values remains computationally intractable in general, motivating the development of various approximation schemes. In this work, we introduce PKeX-Shapley, a novel algorithm that utilizes the multiplicative structure of product kernels to enable the exact computation of Shapley values in polynomial time. We show that product-kernel models admit a functional decomposition that allows for a recursive formulation of Shapley values. This decomposition not only yields computational efficiency but also enhances interpretability in kernel-based learning. We also demonstrate how our framework can be generalized to explain kernel-based statistical discrepancies such as the Maximum Mean Discrepancy (MMD) and the Hilbert-Schmidt Independence Criterion (HSIC), thus offering new tools for interpretable statistical inference.

## 1 Introduction

Shapley values [1], a solution concept originating from cooperative game theory, offer a principled, axiomatic framework for feature attribution in machine learning (ML) [2–4]. Thanks to their rigorous axiomatic foundation, there has been a widespread adoption within explainable AI [5]. They allow a model’s output—such as predictions or losses—to be *fairly* distributed across input features based on their individual and joint contributions. Consequently, several methods have been proposed to estimate Shapley values, ranging from general model-agnostic methods like Kernel SHAP [2] to model-specific methods that leverage structural properties to improve statistical or computational efficiency. Well-known examples of the latter include Tree SHAP for tree-based models [6], GPSHAP for Gaussian processes [7], Deep SHAP for deep networks [2], and, most relevant to our work, RKHS-SHAP for kernel methods [8]. Kernel methods are particularly notable—not only for their use in prediction tasks but also in a broad range of statistical inference problems, including two-sample testing [9–11], goodness-of-fit testing [12, 13], (conditional) independence testing [14], causal inference and discovery [15–18], among others. Hence, as kernel methods gain widespread adoption in high-stakes applications for their flexibility and expressive power, the need for interpretability has become increasingly vital.

Despite their desirable properties, adopting Shapley values in machine learning generally faces two key challenges. The first is defining and estimating a suitable value function that quantifies the contribution of a coalition of features. Ideally, this function should reflect the model’s behavior when the complementary features are absent. A natural approach is to retrain the model on each subset and use the resulting prediction as the value [19]—an approach that is computationally infeasible due to the exponential number of retrains required. A popular alternative simulates feature absence via marginal or conditional expectations of the model’s output, conditioned on the subset being fixed (see Sundararajan and Najmi [5] for other candidates). However, accurately estimating these expectations is difficult, often requiring density estimation or making simplifying assumptions such as feature independence, which often result in misleading and unfaithful explanations [20]. Chau et al. [8] addresses this under the context of kernel methods by utilizing the structure of reproducing kernel Hilbert spaces (RKHS) and adopting kernel distributional embeddings [21] to estimate value functions nonparametrically, thereby avoiding density estimation and independence assumptions.

Given a value function, the second challenge is efficiently estimating the Shapley values. Exact computation requires evaluating the value function over all  $2^d$  possible feature subsets for  $d$  features, which is computationally infeasible. To address this, approximation techniques—such as Monte Carlo sampling and regression-based methods—are commonly used to estimate Shapley values from a smaller set of computed values. While these methods reduce computational costs, they introduce estimation errors that scale with dataset size and feature dimensionality [20]. Model-specific structures can sometimes mitigate this, as in Tree SHAP, which leverages tree decompositions for efficient computation. RKHS-SHAP, however, focuses on improving the statistical estimation of the value function, while Shapley values themselves are still approximated via regression-based methods—thus retaining the limitations mentioned above. Moreover, Chau et al. [8] focuses solely on learning algorithms and does not address the explanation of non-parametric statistical discrepancies, where kernel methods play a central role.

To enhance Shapley value-based attribution for kernel methods, we focus on a subclass that employs product kernels—referred to as product-kernel methods—and introduce PKeX-Shapley (**P**roduct-**K**ernel-based **eX**act **S**hapley attribution). Product kernels are widely used due to their computational efficiency and strong theoretical guarantees. For example, the product of universal kernels remains universal, meaning the resulting RKHS can approximate any continuous function, provided each component kernel is sufficiently expressive [22]. While our focus on product kernels narrows the scope relative to Chau et al. [8], which considers generic kernels, we show that this added structure brings significant benefits in addressing the two aforementioned challenges. First, we demonstrate that product-kernel methods naturally admit a functional decomposition—an additive sum over subsets of features. This motivates our choice of value function of set  $S$ : we accumulate all components  $S'$  from the functional decomposition for all  $S' \subseteq S$ , following ideas similar to those in [23]. Second, leveraging this decomposition, we develop a recursive algorithm that computes exact Shapley values in polynomial time—eliminating the need for sampling or regression-based estimation, and significantly improving computational efficiency over existing methods. Another independent yet important contribution of our work is that we apply our computationally efficient framework to explain kernel-based statistical discrepancies such as the Maximum Mean Discrepancy (MMD) and the Hilbert space Independence Criterion (HSIC), leading to interpretable statistical inference. The Python implementation of this work is available at [24].

## 2 Background

**Notation.** Let  $\mathcal{D}$  denote the set of  $d$  features, and  $2^{\mathcal{D}}$  its power set. The training set  $(\mathbf{x}^{(i)}, y^{(i)})_{i=1}^n$  consists of  $n$  samples, where  $\mathbf{x}^{(i)} \in \mathbb{R}^d$  and  $y^{(i)} \in \mathbb{R}$  (or a discrete label set for classification tasks). Let  $\mathbf{X} \in \mathbb{R}^{n \times d}$  be the matrix of features, and  $\mathbf{X}_S \in \mathbb{R}^{n \times s}$  the submatrix restricted to features in subset  $S \subseteq \mathcal{D}$ , and we write  $\mathbf{X}_j := \mathbf{X}_{\{j\}}$ . We use capital letters for random variables, bold capital letters for matrices, calligraphic letters for sets, and bold lowercase letters for vectors. The restriction of a vector  $\mathbf{x}$  to features in  $S$  is denoted by  $\mathbf{x}_S$ . The elementwise product is denoted by  $\odot$ , and expectation by  $\mathbb{E}$ . A symmetric positive (semi-)definite kernel function over  $\mathcal{D}$  is denoted by  $k$ , and its restriction to subset  $S$  by  $k_S$ . The corresponding kernel matrices are denoted by  $\mathbf{K}$  and  $\mathbf{K}_S$ , respectively. All proofs are provided in Appendix C.

**Shapley value.** The Shapley value [1], rooted in cooperative game theory, is a popular attribution method for computing feature importance in predictive models. It fairly distributes a model’s output

across its input features by (weighted) averaging over their marginal contributions across all possible feature subsets. Specifically, given a value function (or characteristic function)  $v : 2^{\mathcal{D}} \rightarrow \mathbb{R}$ , which quantifies the contribution of a feature subset, the Shapley value for a feature  $j$  is defined as

$$\phi_j = \sum_{S \subseteq \mathcal{D} \setminus \{j\}} \mu(|S|) (v(S \cup \{j\}) - v(S)), \quad (1)$$

where  $\mu(s) = s!(d-s-1)!/d!$  and  $v(S \cup \{j\}) - v(S)$  measures the marginal contribution of feature  $j$  when added to subset  $S$ . The Shapley value is the unique solution satisfying four axioms of efficiency, null player, symmetry, and linearity for any specified value function [1]. However, in the context of explainability, defining this value function  $v$ —which determines how subsets of features contribute to the model’s output—is itself a non-trivial challenge. Several definitions have been proposed [5], but two are widely adopted: the interventional value function  $v_{\mathbf{x}}(S) = \mathbb{E}_{X_{\mathcal{D} \setminus S} | X_S = \mathbf{x}_S} [f(\mathbf{x}_S, X_{\mathcal{D} \setminus S})]$ , which replaces missing features with samples from their marginal distributions [25, 26], and the observational value function  $v_{\mathbf{x}}(S) = \mathbb{E}_{X_{\mathcal{D} \setminus S}} [f(X) | X_S = \mathbf{x}_S]$ , which imputes them using the conditional distribution given observed features [2]. While the observational approach preserves feature dependencies, it requires estimating complex conditional expectations, making it computationally demanding.

Many existing methods estimate value functions by sampling from marginal or conditional distributions, requiring repeated model evaluations that become costly for large models or high-dimensional data [5]. These estimates typically rely on a set of background samples (i.e., a subset of the training data), which can significantly influence the resulting explanations [27, Chapter 21]. Recent kernel-based approaches offer a more (statistically) efficient alternative by using kernel embeddings of marginal or conditional distributions [21] to derive closed-form expressions for nonparametric estimations of value functions in RKHS [8, 7]. While this formulation accelerates value function estimation, the Shapley value itself is still approximated via regression over a subset of feature coalitions, based on the Kernel SHAP [2] formulation.

In this work, we bypass the challenge of estimating value functions by adopting a functional decomposition approach—well-established in classical statistics, particularly in global sensitivity analysis [28] and analysis of variance [29, 30].

**Functional decomposition.** The functional decomposition of a function  $f$  expresses it as a sum of components indexed by subsets of input variables:  $f(\mathbf{x}) = \sum_{S \subseteq \mathcal{D}} f_S(\mathbf{x}_S)$ .

Each term  $f_S(\mathbf{x}_S)$  captures the contribution of a feature subset  $S$  to the function output, reflecting both individual effects and higher-order interactions. This decomposition provides a principled framework for analyzing how input variables influence model predictions. By avoiding the need to estimate expectations and explicitly modeling the influence of feature combinations, it has recently gained significant attention in the explainability literature [23, 31, 32]. Bordt and von Luxburg [23] connect functional decomposition with the Shapley value by defining the value function in terms of the  $f_S$  components, thereby extending SHAP to account for both main effects and higher-order interactions. Fumagalli et al. [31] further explore this connection by analyzing various local and global games derived from functional decompositions, offering a unified perspective on local interpretability (feature attributions for individual predictions) and global interpretability (aggregate contributions across the dataset).

In the next section, we build on this line of work by defining the value function via functional decomposition and showing that, for product-kernel methods, this value function arises naturally. We then introduce a recursive formulation that enables the exact computation of Shapley values in polynomial time—significantly improving over the exponential complexity of standard approaches.

### 3 Exact Shapley value computation for product-kernel learning methods

In this section, we demonstrate how to compute *exact* Shapley values for local explanation in polynomial time when the predictive model is constructed through product-kernel methods, e.g., an SVM or kernel ridge regressor built using product kernels.

### 3.1 Functional decomposition and game-theoretic analysis

Product-kernel methods rely on kernel functions to capture complex relationships between input features and output. A kernel-based decision function is generally expressed as  $f(\mathbf{x}) = \sum_{i=1}^n \alpha_i k(\mathbf{x}, \mathbf{x}^{(i)})$ , where  $k$  is a product kernel function, and  $\alpha_i$  are the learned coefficients associated with the model. The product kernel  $k$  can be expressed as products of base kernels  $k_j, j \in \mathcal{D}$ :

$$k(\mathbf{x}, \mathbf{x}^{(i)}) = \prod_{j \in \mathcal{D}} k_j(x_j, x_j^{(i)}). \quad (2)$$

Product-kernel methods are widely used in machine learning for their simplicity and effectiveness in modeling similarities in high-dimensional data—by designing a kernel for each feature and then multiplying them together [33]. They also come with strong theoretical guarantees: if the base kernels are universal—i.e., capable of approximating any continuous function defined on the marginal input—then the product kernel inherits this property. Specifically, Szabó and Sriperumbudur [22] show that product kernels preserve universality and can approximate any continuous function on the whole domain arbitrarily well. Some well-known kernels, such as the radial basis function (RBF) with an isotropic or anisotropic bandwidth, belong to the family of product kernels, i.e.,  $k(\mathbf{x}, \mathbf{x}') = \exp(-\|\mathbf{x} - \mathbf{x}'\|^2/2\sigma^2) = \prod_{j=1}^d \exp(-(x_j - x'_j)^2/2\sigma^2)$  (see Appendix A for more details on product kernels).

For a product kernel, the decision function naturally induces a functional decomposition.

**Theorem 1.** *A decision function constructed using a product kernel naturally admits a functional decomposition where each component  $f_S(\mathbf{x}_S)$  is given by:*

$$f_S(\mathbf{x}_S) = \sum_{i=1}^n \alpha_i \prod_{j \in S} (k_j(x_j, x_j^{(i)}) - 1). \quad (3)$$

This theorem demonstrates that product-kernel methods induce a functional decomposition with a specific structure. It clarifies how different features contribute to the prediction and interact with each other. Leveraging this functional decomposition, we define  $v_{\mathbf{x}}(S)$  as the aggregate of all components  $f_T(\mathbf{x}_T), \forall T \subseteq S$ , which quantifies the cumulative influence of the coalition  $S$  [23, 31].

**Definition 2.** *For a decomposable function  $f$ , the value function is  $v_{\mathbf{x}}(S) = \sum_{T \subseteq S} f_T(\mathbf{x}_T)$ .*

We now show that this value function can be efficiently computed for product-kernel learning methods.

**Proposition 3.** *For product-kernel learning methods,  $v_{\mathbf{x}}(S)$  can be computed efficiently as*

$$v_{\mathbf{x}}(S) = \boldsymbol{\alpha}^\top k_S(\mathbf{X}_S, \mathbf{x}_S). \quad (4)$$

The value function (4) quantifies the contribution of a feature subset  $S$  by evaluating the kernel function restricted to that subset only. Thus, it isolates the effect of  $S$  by applying the kernel only to those features, ensuring that the contribution of  $S$  is measured independently of the remaining features. Also, computing the value function has linear time complexity, making it highly efficient.

### 3.2 A recursive formulation for Shapley value

Next, we show that for the value function (4), the Shapley value for product-kernel learning methods can be recursively computed in polynomial time.

**Theorem 4.** *Let  $\mathcal{Z} := \{\mathbf{z}_1, \dots, \mathbf{z}_d\}$  with  $\mathbf{z}_i = k_i(\mathbf{X}_i, x_i)$  and  $e_q(\mathcal{Z})$  the elementary symmetric polynomials (ESPs) of order  $q$  over  $\mathcal{Z}$ , defined recursively as  $e_q(\mathcal{Z}_{-j}) = \frac{1}{q} \sum_{r=1}^q (-1)^{r-1} e_{q-r}(\mathcal{Z}_{-j}) \odot p_r(\mathcal{Z}_{-j})$ , where  $p_r(\mathcal{Z}) = \sum_{\mathbf{z}_i \in \mathcal{Z}} \mathbf{z}_i^r$  is the element-wise degree- $r$  power sum. For product-kernel learning methods with coefficients  $\boldsymbol{\alpha}$ , the Shapley value  $\phi_j^{\mathbf{x}}$  for feature  $j$  of instance  $\mathbf{x}$  can then be expressed as*

$$\phi_j^{\mathbf{x}} := \sum_{S \subseteq \mathcal{D} \setminus \{j\}} \mu(|S|) (v_{\mathbf{x}}(S \cup \{j\}) - v_{\mathbf{x}}(S)) = \boldsymbol{\alpha}^\top \left( \left( k_j(\mathbf{X}_j, x_j) - \mathbf{1} \right) \odot \sum_{q=0}^{d-1} \mu(q) e_q(\mathcal{Z}_{-j}) \right). \quad (5)$$

The recursion follows from Newton’s identities for ESPs [34], which we explain further in Appendix B. The intuition to arrive at equation (5) is to use the multiplicative structure of the product kernel to factorize the marginal contribution  $v_{\mathbf{x}}(\mathcal{S} \cup \{j\}) - v_{\mathbf{x}}(\mathcal{S})$  as  $\boldsymbol{\alpha}^\top ((k_j(\mathbf{X}_j, x_j) - 1) \odot k_{\mathcal{S}}(\mathbf{X}_{\mathcal{S}}, \mathbf{x}_{\mathcal{S}}))$ . This structure allows us then to push the summation inside the inner product between the coefficients  $\boldsymbol{\alpha}$  and the kernel evaluations, and express the total sum over all subsets  $\mathcal{S} \subseteq \mathcal{D} \setminus \{j\}$  in terms of weighted ESPs  $e_q(\mathcal{Z}_{-j})$ , which can then be computed recursively in  $O(d^2)$ . A similar trick has been used in the context of additive Gaussian processes [35], but to our knowledge, it has not been previously leveraged for computing Shapley values in polynomial time. We present the algorithm in Appendix D, along with a modification that is numerically stable.

Next, we show the additivity of the explanation for the value function in equation (4) (see Appendix E for discussion on the additivity of explanations for different values for the null game).

**Lemma 5.** *For any instance  $\mathbf{x}$ , the sum of Shapley values satisfies:  $\sum_{j=1}^d \phi_j^{\mathbf{x}} = f(\mathbf{x}) - f_{\emptyset}(\mathbf{x})$  where  $f_{\emptyset}(\mathbf{x}) = \sum_{i=1}^n \alpha_i$  represents the baseline contribution with no features.*

## 4 Explaining kernel-based statistical discrepancies

This section demonstrates the interpretation of the two kernel-based statistical discrepancies, HSIC and MMD, with product kernels. We discuss the additivity of the explanations in Appendix E.

### 4.1 Distributing the discrepancy: Explaining MMD

The *Maximum Mean Discrepancy* (MMD) quantifies the difference between two probability distributions in terms of their kernel mean embeddings:  $\text{MMD}^2(\mathbb{P}, \mathbb{Q}) := \|\mu_{\mathbb{P}} - \mu_{\mathbb{Q}}\|_{\mathcal{H}_k}^2$  where  $\mathcal{H}_k$  is the RKHS associated with the kernel  $k$  and  $\mu_{\mathbb{P}} := \int k(\mathbf{x}, \cdot) d\mathbb{P}(\mathbf{x}) \in \mathcal{H}_k$  is the kernel mean embedding of  $\mathbb{P}$  [21, Sec. 3.5]. The embedding  $\mu_{\mathbb{Q}}$  is defined analogously. Based on the samples  $\{\mathbf{x}^{(i)}\}_{i=1}^n \sim \mathbb{P}$  and  $\{\mathbf{z}^{(i)}\}_{i=1}^m \sim \mathbb{Q}$ , the empirical estimate of MMD, expressed entirely in terms of  $k$ , is given by

$$\widehat{\text{MMD}}^2(\mathbb{P}, \mathbb{Q}) = \frac{1}{n(n-1)} \sum_{i \neq j} k(\mathbf{x}^{(i)}, \mathbf{x}^{(j)}) + \frac{1}{m(m-1)} \sum_{i \neq j} k(\mathbf{z}^{(i)}, \mathbf{z}^{(j)}) - \frac{2}{nm} \sum_{i,j} k(\mathbf{x}^{(i)}, \mathbf{z}^{(j)}).$$

In this section, we propose an attribution method to allocate the overall discrepancy measured by MMD among the involved variables. Such an attribution is useful in many problems, including explaining MMD-based statistics for hypothesis testing (e.g., Gretton et al. [9]) and determining the contribution of variables to covariance shift (e.g., Zhang et al. [36]). By analyzing MMD through a game-theoretic perspective, we uncover its functional decomposition structure, which facilitates the formulation of a cooperative game under the assumption that  $k$  is a product kernel.

**Theorem 6.** *The MMD with a product kernel has the following properties:*

(i) *The MMD function can be decomposed into contributions from all feature subsets  $\mathcal{S} \subseteq \mathcal{D}$  as*

$$\begin{aligned} \widehat{\text{MMD}}^2(\mathbb{P}, \mathbb{Q}) &= \sum_{\mathcal{S} \subseteq \mathcal{D}} \left[ \frac{1}{n(n-1)} \sum_{i \neq j} \prod_{q \in \mathcal{S}} (k_q(x_q^{(i)}, x_q^{(j)}) - 1) \right. \\ &\quad \left. + \frac{1}{m(m-1)} \sum_{i \neq j} \prod_{q \in \mathcal{S}} (k_q(z_q^{(i)}, z_q^{(j)}) - 1) - \frac{2}{nm} \sum_{i,j} \prod_{q \in \mathcal{S}} (k_q(x_q^{(i)}, z_q^{(j)}) - 1) \right]. \end{aligned}$$

(ii) *Given this decomposition, the corresponding value function, which represents the contribution of the variables in  $\mathcal{S}$ , is uniquely defined as follows:  $v_{\text{MMD}}(\mathcal{S}) = \frac{1}{n(n-1)} \sum_{i \neq j} k_{\mathcal{S}}(\mathbf{x}_{\mathcal{S}}^{(i)}, \mathbf{x}_{\mathcal{S}}^{(j)}) + \frac{1}{m(m-1)} \sum_{i \neq j} k_{\mathcal{S}}(\mathbf{z}_{\mathcal{S}}^{(i)}, \mathbf{z}_{\mathcal{S}}^{(j)}) - \frac{2}{nm} \sum_{i,j} k_{\mathcal{S}}(\mathbf{x}_{\mathcal{S}}^{(i)}, \mathbf{z}_{\mathcal{S}}^{(j)})$ .*

By applying the same trick as in Theorem 4 to the value function  $v_{\text{MMD}}$ , we can obtain a similar recursive formulation of Shapley values for MMD. That is, for the first term in  $v_{\text{MMD}}$ , we use the multiplicate structure of product kernels and write  $v_{\text{MMD}}(\mathcal{S} \cup \{q\}) - v_{\text{MMD}}(\mathcal{S})$  as  $k_{\mathcal{S} \cup \{q\}}(\mathbf{x}_{\mathcal{S} \cup \{q\}}^{(i)}, \mathbf{x}_{\mathcal{S} \cup \{q\}}^{(j)}) - k_{\mathcal{S}}(\mathbf{x}_{\mathcal{S}}^{(i)}, \mathbf{x}_{\mathcal{S}}^{(j)}) = (k_q(x_q^{(i)}, x_q^{(j)}) - 1) k_{\mathcal{S}}(\mathbf{x}_{\mathcal{S}}^{(i)}, \mathbf{x}_{\mathcal{S}}^{(j)})$ . By pushing out  $k_q(x_q^{(i)}, x_q^{(j)}) - 1$  from the summation in the Shapley value, we can express the total sum over  $\mathcal{S} \subseteq \mathcal{D} \setminus \{q\}$  as the weighted ESPs. The following proposition summarizes this.

**Proposition 7.** Let  $\mathcal{Z}(\mathbf{x}, \mathbf{x}') = \{k_1(x_1, x'_1), \dots, k_d(x_d, x'_d)\}$ , and  $e_r(\mathcal{Z}(\mathbf{x}, \mathbf{x}'))$  determined as

$$e_r(\mathcal{Z}_{-q}(\mathbf{x}, \mathbf{x}')) = \frac{1}{r} \sum_{s=1}^r (-1)^{s-1} e_{r-s}(\mathcal{Z}_{-q}(\mathbf{x}, \mathbf{x}')) p_s(\mathcal{Z}_{-q}(\mathbf{x}, \mathbf{x}')),$$

where  $p_s(\mathcal{Z}) = \sum_{z \in \mathcal{Z}} z^s$  represents the degree- $s$  power sum. Further, let  $\gamma_q(\mathbf{x}, \mathbf{x}')$  be defined as  $\gamma_q(\mathbf{x}, \mathbf{x}') := (k_q(x_q, x'_q) - 1) \sum_{r=0}^{d-1} \mu(r) e_r(\mathcal{Z}_{-q}(\mathbf{x}, \mathbf{x}'))$ . Then, for product kernels, the Shapley value for the MMD can be recursively computed as

$$\phi_q^{MMD} = \frac{1}{n(n-1)} \sum_{i \neq j} \gamma_q(\mathbf{x}^{(i)}, \mathbf{x}^{(j)}) + \frac{1}{m(m-1)} \sum_{i \neq j} \gamma_q(\mathbf{z}^{(i)}, \mathbf{z}^{(j)}) - \frac{2}{nm} \sum_{i,j} \gamma_q(\mathbf{x}^{(i)}, \mathbf{z}^{(j)}).$$

The Shapley values  $\phi_q^{MMD}$  allow us to allocate the overall distributional discrepancy between  $\mathbb{P}$  and  $\mathbb{Q}$  across the variables, identifying the most influential ones in distinguishing the two distributions.

## 4.2 Distributing the dependence: Explaining HSIC

The *Hilbert-Schmidt Independence Criterion* (HSIC) is a kernel-based dependence measure that quantifies the statistical dependence between two random variables. Let  $X$  and  $Y$  be two random variables with  $k(\cdot, \cdot)$  and  $l(\cdot, \cdot)$  as reproducing (product) kernels defined on them. Then,  $\text{HSIC}(X, Y) := \|\mathcal{C}_{XY}\|_{\text{HS}}^2$ , where  $\mathcal{C}_{XY}$  is the cross-covariance operator and  $\|\cdot\|_{\text{HS}}$  is the Hilbert-Schmidt (HS) norm; see, e.g., [21, Sec. 3.6] for technical details. Given a sample  $\{(\mathbf{x}^{(i)}, \mathbf{y}^{(i)})\}_{i=1}^n \sim \mathbb{P}(X, Y)$ ,  $\text{HSIC}(X, Y)$  can be estimated as  $\widehat{\text{HSIC}}(X, Y) = (n-1)^{-2} \text{tr}(\mathbf{KHLH})$  where  $\mathbf{K} \in \mathbb{R}^{n \times n}$  is the kernel matrix computed using the kernel  $k$ , i.e.,  $\mathbf{K}_{ij} = k(\mathbf{x}^{(i)}, \mathbf{x}^{(j)})$ ,  $\mathbf{L} \in \mathbb{R}^{n \times n}$  is the kernel matrix computed using the kernel  $l$ , i.e.,  $\mathbf{L}_{ij} = l(\mathbf{y}^{(i)}, \mathbf{y}^{(j)})$ , and  $\mathbf{H} = I - \frac{1}{n} \mathbf{1}\mathbf{1}^\top$  is the centering matrix ensuring zero mean in the feature space.

Computing  $\text{HSIC}(X, Y)$  gives us the overall dependence between  $X$  and  $Y$ . We now focus on scenarios where  $X$  represents a random variable of the feature vector  $\mathbf{x}$  and  $Y$  represents the scalar prediction outcome  $y$ . Our interest is then to distribute the overall dependence over the features in  $\mathbf{x}$ . This is particularly useful for feature selection and global sensitivity analysis, where the target is usually univariate.

The following theorem establishes that HSIC naturally induces a functional decomposition structure, enabling the formulation of a cooperative game.

**Theorem 8.** For the HSIC with the product kernel on  $X$ , it has the following properties:

(i) The HSIC function can be decomposed into contributions from all feature subsets  $\mathcal{S} \subseteq \mathcal{D}$  as

$$\widehat{\text{HSIC}}(X, Y) = \frac{1}{(n-1)^2} \sum_{\mathcal{S} \subseteq \mathcal{D}} \text{tr} \left( \mathbf{HLH} \odot (\mathbf{K}_{\mathcal{S}} - \mathbf{1}\mathbf{1}^\top) \right).$$

(ii) Given this decomposition, the associated value function that quantifies the contribution of the variable set  $\mathcal{S}$  to the overall dependency is uniquely defined as  $v_{\text{HSIC}}(\mathcal{S}) = (n-1)^{-2} \text{tr}(\mathbf{HLHK}_{\mathcal{S}})$ .

Applying the same trick as in Proposition 7 to the value function  $v_{\text{HSIC}}$  yields a similar recursive formulation of Shapley values for HSIC.

**Proposition 9.** For the product kernel, the Shapley value for HSIC can be recursively computed as:

$$\phi_j^{\text{HSIC}} = \frac{1}{(n-1)^2} \text{tr} \left( \mathbf{HLH} \left( (\mathbf{K}_j - \mathbf{1}\mathbf{1}^\top) \odot \sum_{q=0}^{d-1} \mu(q) E_q(\mathcal{K}_{-j}) \right) \right).$$

where  $\mathcal{K} = \{\mathbf{K}_1, \dots, \mathbf{K}_d\}$  with  $\mathbf{K}_i$  being the kernel matrix for feature  $i$  only, and  $E_q(\mathcal{K}_{-j}) = \frac{1}{q} \sum_{r=1}^q (-1)^{r-1} E_{q-r}(\mathcal{K}_{-j}) \odot P_r(\mathcal{K}_{-j})$ , is the ESPs with  $P_r(\mathcal{K}) = \sum_{\mathbf{K}_i \in \mathcal{K}} \mathbf{K}_i^r$  being the element-wise degree- $r$  power sum.

The Shapley values  $\phi_j^{\text{HSIC}}$  allow us to allocate the overall dependence between  $X$  and  $Y$  across individual features fairly, identifying the most influential ones for prediction. Our results can be generalized to scenarios when both  $X$  and  $Y$  are multivariate; see Appendix F for further details. The attribution of overall dependence to the involved multivariate variables has other applications in statistical inference as well, e.g., kernel-based (conditional) independence testing [14, 37].

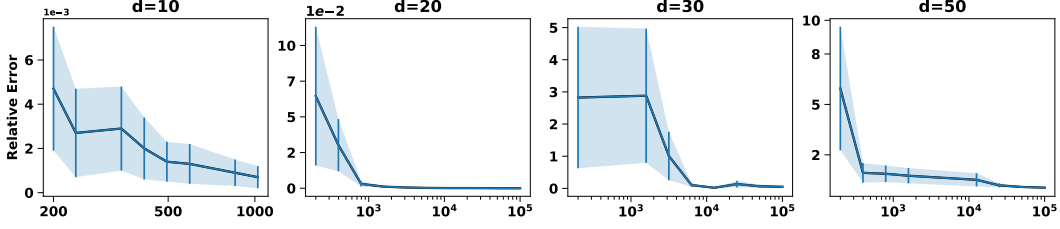


Figure 1: Relative estimation error of regression-based Shapley values versus the exact recursive values, shown across coalition sample sizes for feature dimensions  $d = 10, 20, 30, 50$ .

## 5 Experiments

We evaluate the effectiveness of PKeX-Shapley for product-kernel methods through a series of experiments conducted on a 24-core machine with 16GB RAM and an RTX4000 GPU. We further provide the experimental setups, training procedure, and extra experiments in Appendix G.

### 5.1 Demonstrating the effectiveness of recursion and the value function via local explanations

**Experiment 1: Recursion vs. Regression Formulation.** We empirically demonstrate the advantage of PKeX-Shapley, compared to sampling-based approximations such as Kernel SHAP. We generate four synthetic datasets, each with 1000 samples and  $d \in \{10, 20, 30, 50\}$  features. Features are independently drawn from a standard normal distribution, and target values are generated using a linear model with additive Gaussian noise ( $\sigma = 0.1$ ). For each dataset, we train a support vector regression model with an RBF kernel and use the trained model to compare explanation methods.

For a fair comparison between the recursive and regression-based methods, we adopt the same value function as defined in Definition 2. Specifically, we first compute the exact Shapley values  $\phi_j^x$  using PKeX-Shapley, and then estimate the Shapley values using a regression-based approach analogous to Kernel SHAP, but modified to employ our value function from Definition 2. The estimator uses the paired coalition sampling scheme of Covert and Lee [38], with sample sizes ranging from 200 to  $10^5$ , and computes  $\hat{\phi}_j^x$  by solving the corresponding weighted linear regression problem. To quantify the approximation error introduced by the regression formulation, we report the relative deviation error across 100 randomly selected instances, defined as  $\sum_{j=1}^d |\phi_j^x - \hat{\phi}_j^x| / |\phi_j^x|$ .

Figure 1 plots the relative error as a function of sample size for each dataset over the 100 selected instances. When  $d = 10$ , the relative error is already around 0.005 with 200 coalition samples ( $\approx 20\%$  of all possible coalitions). However, when  $d = 50$ , the approximation error remains above 9.0 with 200 samples, stays above 1.0 with  $10^4$ , and only approaches 0.05 near  $10^5$  coalition samples. These results highlight that as the number of features increases, a substantially larger number of samples is required to obtain reliable estimates—rendering sampling-based methods impractical in high-dimensional settings. This demonstrates the advantage of our exact recursive computation.

**Experiment 2: Effectiveness of the Functional-Decomposition-Based Value Function.** Recall that PKeX-Shapley employs a value function based on functional decomposition, in contrast to standard expectation-based value functions. It is therefore natural to ask whether this formulation meaningfully captures the importance of feature subsets. To evaluate this, we assess the quality of the resulting explanations in recovering the most informative feature on synthetic datasets, and compare PKeX-Shapley against alternative explanation methods. We generate three regression tasks of  $n = 1000$  samples in  $\mathbb{R}^{50}$ , where only the first one-third of features (denoted by  $S$ ,  $|S| = 17$ ) drive the target, and the remaining 33 features are redundant. The three target functions over  $S$  are: a degree-5 polynomial, a degree-10 polynomial, and a squared-exponential response  $y = \exp(\sum_{i \in S} x_i^2)$ . We train a support vector regressor with an RBF kernel on each dataset, and produce explanations using our exact recursive method alongside three baselines: RKHS-SHAP [8], GEMFIX [39], BiSHAP [40], and Sampling SHAP [41], each configured with 500 and 1000 coalition samples. All methods employ a fixed background set of 100 points to estimate their value functions.

Attribution accuracy is computed over 100 independent test instances by selecting the top-17 features returned by each method and measuring the fraction of true active features recovered. Figure 2 shows the average accuracy rate for each method across the three tasks. PKeX-Shapley achieves a competitive or superior performance in all cases, whereas Kernel SHAP, GEMFIX, and Sampling

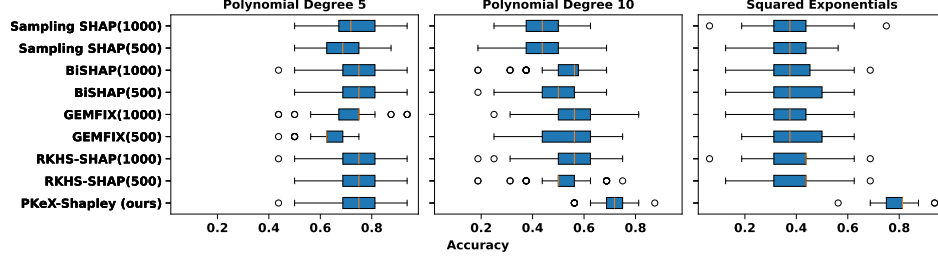


Figure 2: Recovery rate of true active features by each method on the three synthetic tasks.

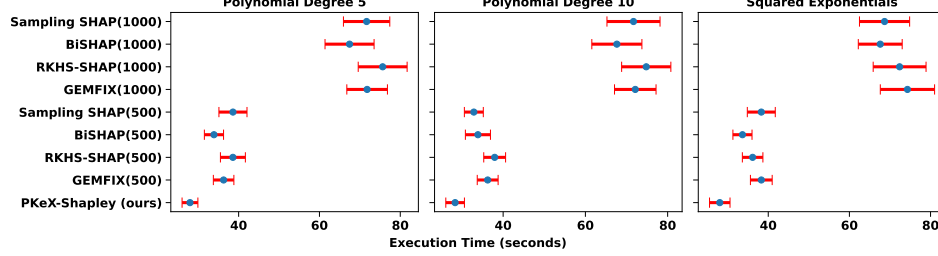


Figure 3: Per-instance explanation time (mean  $\pm$  standard deviation) for each method with 500 and 1000 coalition samples.

SHAP suffer accuracy degradation as the target function’s complexity increases (most notably for degree-10 polynomial and the exponential model).

We also measure per-instance explanation runtime. Figure 3 presents error-bar plots (mean  $\pm$  standard deviation) of execution times in seconds. With 500 coalition samples, all methods incur comparable execution times. When the sample size increases to 1000, PKeX-Shapley remains significantly faster than the baselines, despite using the same background-sample budget of 100 for other methods. This demonstrates that PKeX-Shapley not only provides exact attributions but also outperforms sampling-based estimators in computational efficiency as coalition sample counts grow.

## 5.2 Explaining distribution discrepancy using MMD with PKeX-Shapley

To illustrate how PKeX-Shapley can explain distributional discrepancies measured by MMD, we conduct two synthetic experiments following the standard two-sample testing setup [10]. Our goal is to attribute the observed MMD between two distributions to individual input variables. We present one of the synthetic experiments below, with the remaining experiments provided in Appendix G.2. In all MMD experiments, we use the RBF kernel with the bandwidth selected via the median heuristic.

We generate datasets  $X$  and  $Z$ , each comprising 20 variables. The first ten variables  $X_1, \dots, X_{10}$  and  $Z_1, \dots, Z_{10}$  are sampled from the same multivariate normal distribution, ensuring identical distributions. The remaining 10 variables  $X_{11}, \dots, X_{20}$  differ, with variables in  $X$  sampled from a multivariate normal distribution and those in  $Z$  from a Student’s t-distribution of the same mean. This introduces differences in higher-order moments and covariance structure, resulting in a measurable discrepancy.

We generate 1,000 samples from each distribution and compute the MMD. Shapley values are computed to quantify the contribution of each variable to the overall MMD. To ensure robustness, the experiment was repeated 1,000 times, and kernel density estimates (KDE) of the Shapley values are presented in Figure 4.

The left subplot in Figure 4 displays the KDE plots for variables 1–10, while the right subplot corresponds to variables 11–20. For the first 10 variables, the consistently negative Shapley

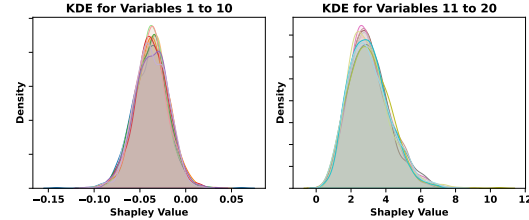


Figure 4: KDE plots of Shapley values for the synthetic dataset. Variables 1–10 reduce MMD via negative contributions, while 11–20 increase it via positive contributions.



Table 1: Performance (mean $\pm$ standard deviation) when training on the top 20% of features. Datasets *breast cancer*, *skillcraft*, *sml*, and *parkinson* are regression (MAPE, lower is better); *sonar*, *Wisconsin*, *ionosphere* are classification (accuracy, higher is better).

Method	sonar	Wisconsin	ionosphere	breast cancer	skillcraft	sml	parkinson
	accuracy ( $\uparrow$ )			mean absolute percentage error ( $\downarrow$ )			
PKeX-Shapley	0.808 $\pm$ 0.030	<b>0.909<math>\pm</math>0.015</b>	0.878 $\pm$ 0.036	<b>0.850<math>\pm</math>0.010</b>	<b>1.000<math>\pm</math>0.020</b>	0.999 $\pm$ 0.001	<b>0.125<math>\pm</math>0.022</b>
HSICLasso	0.808 $\pm$ 0.044	0.884 $\pm$ 0.010	0.912 $\pm$ 0.035	1.000 $\pm$ 0.080	2.175 $\pm$ 0.429	1.354 $\pm$ 0.726	1.170 $\pm$ 0.269
MI	<b>0.875<math>\pm</math>0.053</b>	0.900 $\pm$ 0.015	<b>0.937<math>\pm</math>0.023</b>	1.000 $\pm$ 0.080	1.134 $\pm$ 0.099	<b>0.196<math>\pm</math>0.071</b>	0.214 $\pm$ 0.004
Lasso	0.842 $\pm$ 0.038	0.900 $\pm$ 0.024	0.932 $\pm$ 0.021	1.000 $\pm$ 0.080	1.821 $\pm$ 0.680	1.000 $\pm$ 0.000	1.000 $\pm$ 0.000
K-Best	0.779 $\pm$ 0.040	<b>0.909<math>\pm</math>0.015</b>	0.869 $\pm$ 0.018	1.000 $\pm$ 0.080	1.134 $\pm$ 0.099	0.257 $\pm$ 0.086	1.018 $\pm$ 0.076
Tree Ens.	0.837 $\pm$ 0.059	0.887 $\pm$ 0.033	0.926 $\pm$ 0.031	1.000 $\pm$ 0.080	2.175 $\pm$ 0.429	1.000 $\pm$ 0.000	0.214 $\pm$ 0.004

values indicate a reduction in the overall MMD, effectively “pulling” the discrepancy closer to zero. This aligns with our intuition: since these variables are identically distributed across both datasets, they should not contribute positively to the observed distributional difference. In contrast, variables 11–20 exhibit positive Shapley values, reflecting their contribution to the increase in MMD and, thus, their role in capturing the divergence between the distributions. Moreover, the KDE plots of the Shapley values within each group (variables 1–10 and 11–20, respectively) are nearly identical, which is consistent with the symmetric construction of the synthetic data. This experiment illustrates that Shapley values provide meaningful insights into the contribution of individual variables to distributional discrepancies measured by MMD.

### 5.3 Explaining HSIC with PKeX-Shapley: Feature selection case study

Lastly, we demonstrate how attributing the HSIC between input features and the target variable to individual features can support feature selection by quantifying their respective contributions to the overall statistical dependence. As a comparison, we also compare our approach with five feature importance methods: HSICLasso [42], Mutual Information (MI), Lasso, K-Best, and Tree Ensemble (with feature permutations). Our experiments were conducted on seven datasets, where we trained Gaussian process (GP) models with an RBF kernel, using only the top 20% of features ranked by each selection method.

Table 1 presents the results, reporting the five-fold cross-validated mean and standard deviation for the GP models trained on the selected features. We use mean absolute percentage error (MAPE) as the performance metric for regression tasks and accuracy for classification tasks. For kernel computation in HSIC, we use an RBF kernel for features and regression targets, and a categorical kernel for classification targets. The bandwidth for the RBF kernel is selected using the median heuristic. PKeX-Shapley consistently delivers strong results across all datasets. On regression problems, it yields better MAPE on datasets *breast cancer*, *skillcraft*, and *parkinson*, while other methods often incur higher error (e.g., HSICLasso on *skillcraft* and *parkinson*) or greater variance (e.g., HSICLasso on *sml*). For classification, PKeX-Shapley maintains accuracies above 80%, matching or exceeding the baselines. It achieves the best-performing results on the *Wisconsin* datasets, and remains competitive on the other two datasets. Interestingly, when compared to HSICLasso—a method specifically tailored for feature selection—PKeX-Shapley demonstrates superior performance across the majority of datasets. Notably, we achieve better results in 5 out of the 7 datasets, tie in one, and only fall short in the *ionosphere* dataset. This is particularly noteworthy, as PKeX-Shapley is not explicitly designed for feature selection, yet it consistently outperforms a specialized method like HSICLasso.

## 6 Conclusion, limitation, and discussion

This work introduces PKeX-Shapley, a polynomial-time algorithm for computing exact Shapley values in product-kernel methods. We show that product kernels naturally induce a functional decomposition, which we exploit to develop a recursive algorithm that avoids the exponential complexity of naive Shapley value computation. This approach enables exact, efficient feature attribution for both predictive models and kernel-based statistical discrepancies, including Maximum Mean Discrepancy (MMD) and Hilbert-Schmidt Independence Criterion (HSIC), providing interpretability of distribu-

tional differences and dependence structures. Our method achieves quadratic-time complexity and eliminates the approximation errors inherent in sampling-based estimators (and expectation-based value functions), as demonstrated through experiments on both synthetic and real-world datasets.

While our algorithm reduces computational complexity from exponential to quadratic time, its main limitation is that it applies only to product kernels. This trade-off is largely unavoidable: achieving tractable computation requires imposing structural constraints. As part of future work, we plan to explore whether further relaxation is possible. Another promising direction is to extend our approach to higher-order attribution methods, such as Shapley interaction indices [43, 44]. It is also of interest to investigate connections between our functional decomposition and other explanation techniques, such as partial dependence plots.

## Acknowledgement

This project is funded by the Federal Ministry of Education and Research (BMBF). The DAAD Postdoc-NeT-AI short-term research visit scholarship partially supported the first author.

## References

- [1] Lloyd S Shapley. A value for n-person games. 1953.
- [2] Scott M Lundberg and Su-In Lee. A unified approach to interpreting model predictions. *Advances in neural information processing systems*, 30, 2017.
- [3] Anupam Datta, Shayak Sen, and Yair Zick. Algorithmic transparency via quantitative input influence: Theory and experiments with learning systems. In *2016 IEEE symposium on security and privacy (SP)*, pages 598–617. IEEE, 2016.
- [4] Ian Covert, Scott M Lundberg, and Su-In Lee. Understanding global feature contributions with additive importance measures. *Advances in Neural Information Processing Systems*, 33: 17212–17223, 2020.
- [5] Mukund Sundararajan and Amir Najmi. The many shapley values for model explanation. In *International conference on machine learning*, pages 9269–9278. PMLR, 2020.
- [6] Scott M Lundberg, Gabriel Erion, Hugh Chen, Alex DeGrave, Jordan M Prutkin, Bala Nair, Ronit Katz, Jonathan Himmelfarb, Nisha Bansal, and Su-In Lee. From local explanations to global understanding with explainable ai for trees. *Nature machine intelligence*, 2(1):56–67, 2020.
- [7] Siu Lun Chau, Krikamol Muandet, and Dino Sejdinovic. Explaining the uncertain: Stochastic shapley values for gaussian process models. *Advances in Neural Information Processing Systems*, 36, 2024.
- [8] Siu Lun Chau, Robert Hu, Javier Gonzalez, and Dino Sejdinovic. Rkhs-shap: Shapley values for kernel methods. *Advances in neural information processing systems*, 35:13050–13063, 2022.
- [9] Arthur Gretton, Karsten M Borgwardt, Malte J Rasch, Bernhard Schölkopf, and Alexander Smola. A kernel two-sample test. *The Journal of Machine Learning Research*, 13(1):723–773, 2012.
- [10] Antonin Schrab. A unified view of optimal kernel hypothesis testing. *arXiv preprint arXiv:2503.07084*, 2025.
- [11] Siu Lun Chau, Antonin Schrab, Arthur Gretton, Dino Sejdinovic, and Krikamol Muandet. Credal two-sample tests of epistemic uncertainty. In *International Conference on Artificial Intelligence and Statistics*, pages 127–135. PMLR, 2025.
- [12] Kacper Chwialkowski, Heiko Strathmann, and Arthur Gretton. A kernel test of goodness of fit. In Maria Florina Balcan and Kilian Q. Weinberger, editors, *Proceedings of The 33rd International Conference on Machine Learning*, volume 48 of *Proceedings of Machine Learning Research*, pages 2606–2615, 2016.
- [13] Qiang Liu, Jason Lee, and Michael Jordan. A kernelized stein discrepancy for goodness-of-fit tests. In Maria Florina Balcan and Kilian Q. Weinberger, editors, *Proceedings of The 33rd International Conference on Machine Learning*, volume 48, pages 276–284, 2016.
- [14] Mélisande Albert, Béatrice Laurent, Amandine Marrel, and Anouar Meynaoui. Adaptive test of independence based on hsc measures. *The Annals of Statistics*, 50(2):858–879, 2022.
- [15] Jovana Mitrovic, Dino Sejdinovic, and Yee Whye Teh. Causal inference via kernel deviance measures. *Advances in neural information processing systems*, 31, 2018.
- [16] Daniele Marinazzo, Mario Pellicoro, and Sebastiano Stramaglia. Kernel method for nonlinear granger causality. *Physical review letters*, 100(14):144103, 2008.

- [17] Siu Lun Chau, Jean-Francois Ton, Javier González, Yee Teh, and Dino Sejdinovic. Bayesimp: Uncertainty quantification for causal data fusion. *Advances in Neural Information Processing Systems*, 34:3466–3477, 2021.
- [18] Dino Sejdinovic. An overview of causal inference using kernel embeddings. *arXiv preprint arXiv:2410.22754*, 2024.
- [19] Stan Lipovetsky and Michael Conklin. Analysis of regression in game theory approach. *Applied stochastic models in business and industry*, 17(4):319–330, 2001.
- [20] I Elizabeth Kumar, Suresh Venkatasubramanian, Carlos Scheidegger, and Sorelle Friedler. Problems with shapley-value-based explanations as feature importance measures. In *International conference on machine learning*, pages 5491–5500. PMLR, 2020.
- [21] Krikamol Muandet, Kenji Fukumizu, Bharath Sriperumbudur, Bernhard Schölkopf, et al. Kernel mean embedding of distributions: A review and beyond. *Foundations and Trends® in Machine Learning*, 10(1-2):1–141, 2017.
- [22] Zoltán Szabó and Bharath K Sriperumbudur. Characteristic and universal tensor product kernels. *Journal of Machine Learning Research*, 18(233):1–29, 2018.
- [23] Sebastian Bordt and Ulrike von Luxburg. From shapley values to generalized additive models and back. In *International Conference on Artificial Intelligence and Statistics*, pages 709–745. PMLR, 2023.
- [24] Pkex-shapley: Reproducibility code for neurips 2025 submission. <https://anonymous.4open.science/r/PKeX-Shapley-B1C0/>, 2025.
- [25] Dominik Janzing, Lenon Minorics, and Patrick Blöbaum. Feature relevance quantification in explainable ai: A causal problem. In *International Conference on artificial intelligence and statistics*, pages 2907–2916. PMLR, 2020.
- [26] Tom Heskes, Evi Sijben, Ioan Gabriel Bucur, and Tom Claassen. Causal shapley values: Exploiting causal knowledge to explain individual predictions of complex models. *Advances in neural information processing systems*, 33:4778–4789, 2020.
- [27] Christoph Molnar. *Interpreting Machine Learning Models with SAP: A Guide with Python Examples and Theory on Shapley Values*. Chistoph Molnar c/o MUCBOOK, Heidi Seibold, 2023.
- [28] Art B Owen. Sobol’ indices and shapley value. *SIAM/ASA Journal on Uncertainty Quantification*, 2(1):245–251, 2014.
- [29] Art B Owen. Variance components and generalized sobol’ indices. *SIAM/ASA Journal on Uncertainty Quantification*, 1(1):19–41, 2013.
- [30] Benjamin Lengerich, Sarah Tan, Chun-Hao Chang, Giles Hooker, and Rich Caruana. Purifying interaction effects with the functional anova: An efficient algorithm for recovering identifiable additive models. In Silvia Chiappa and Roberto Calandra, editors, *Proceedings of the Twenty Third International Conference on Artificial Intelligence and Statistics*, volume 108 of *Proceedings of Machine Learning Research*, pages 2402–2412. PMLR, 26–28 Aug 2020.
- [31] Fabian Fumagalli, Maximilian Muschalik, Eyke Hüllermeier, Barbara Hammer, and Julia Herbinger. Unifying feature-based explanations with functional anova and cooperative game theory. *arXiv preprint arXiv:2412.17152*, 2024.
- [32] Munir Hiabu, Joseph T Meyer, and Marvin N Wright. Unifying local and global model explanations by functional decomposition of low dimensional structures. In *International conference on artificial intelligence and statistics*, pages 7040–7060. PMLR, 2023.
- [33] Jacob Gardner, Geoff Pleiss, Ruihan Wu, Kilian Weinberger, and Andrew Wilson. Product kernel interpolation for scalable gaussian processes. In *International Conference on Artificial Intelligence and Statistics*, pages 1407–1416. PMLR, 2018.

- [34] Eric S Egge. *An introduction to symmetric functions and their combinatorics*, volume 91. American Mathematical Soc., 2019.
- [35] David K Duvenaud, Hannes Nickisch, and Carl Rasmussen. Additive gaussian processes. *Advances in neural information processing systems*, 24, 2011.
- [36] Wenju Zhang, Xiang Zhang, Long Lan, and Zhigang Luo. Maximum mean and covariance discrepancy for unsupervised domain adaptation. *Neural Processing Letters*, 51:347–366, 2020.
- [37] Arthur Gretton, Kenji Fukumizu, Choon Teo, Le Song, Bernhard Schölkopf, and Alex Smola. A kernel statistical test of independence. *Advances in neural information processing systems*, 20, 2007.
- [38] Ian Covert and Su-In Lee. Improving kernelshap: Practical shapley value estimation using linear regression. In *International Conference on Artificial Intelligence and Statistics*, pages 3457–3465. PMLR, 2021.
- [39] Majid Mohammadi, Ilaria Tiddi, and Annette Ten Teije. Unlocking the game: Estimating games in möbius representation for explanation and high-order interaction detection. In *Proceedings of the AAAI Conference on Artificial Intelligence*, volume 39, pages 19512–19519, 2025.
- [40] Aria Masoomi, Davin Hill, Zhonghui Xu, Craig P Hersh, Edwin K Silverman, Peter J Castaldi, Stratis Ioannidis, and Jennifer Dy. Explanations of black-box models based on directional feature interactions. In *International Conference on Learning Representations*, 2021.
- [41] Erik Štrumbelj and Igor Kononenko. Explaining prediction models and individual predictions with feature contributions. *Knowledge and information systems*, 41:647–665, 2014.
- [42] Héctor Climente-González, Chloé-Agathe Azencott, Samuel Kaski, and Makoto Yamada. Block hsc lasso: model-free biomarker detection for ultra-high dimensional data. *Bioinformatics*, 35(14):i427–i435, 2019.
- [43] Mukund Sundararajan, Kedar Dhamdhere, and Ashish Agarwal. The shapley taylor interaction index. In *International conference on machine learning*, pages 9259–9268. PMLR, 2020.
- [44] Maximilian Muschalik, Hubert Baniecki, Fabian Fumagalli, Patrick Kolpaczki, Barbara Hammer, and Eyke Hüllermeier. shapiq: Shapley interactions for machine learning. *Advances in Neural Information Processing Systems*, 37:130324–130357, 2024.
- [45] Takuya Akiba, Shotaro Sano, Toshihiko Yanase, Takeru Ohta, and Masanori Koyama. Optuna: A next-generation hyperparameter optimization framework. In *Proceedings of the 25th ACM SIGKDD international conference on knowledge discovery & data mining*, pages 2623–2631, 2019.

## Appendix

The appendix provides additional information and proofs related to the material presented in the main paper. It includes detailed explanations, proofs, algorithms, and experiments relevant to explaining product-kernel models. The structure of the appendix is as follows:

- **Product kernels in kernel methods:** §A discusses the construction and examples of product kernels, including their definitions and properties.
- **Newton’s identities :** §B presents the main result of Newton’s identities for elementary symmetric polynomials.
- **Proofs:** §C provides detailed proofs of key theorems and lemmas used in the main paper.
- **Recursive and numerically stable algorithms for computing Shapley values for product-kernel learning models:** §D describes a recursive algorithm for computing Shapley values, as well as an adjusted algorithm for numerical stability and efficiency.
- **Additivity of explanations for learning models, MMD and HSIC:** §E discusses the additivity of explanations for the product-kernel methods studied in this paper.
- **Shapley value attribution for HSIC with two multivariate variables** §F discusses the Shapley value attribution for HSIC when both random variables are multivariate.
- **Experiments:** §G reports experimental setup and extra experiments on explaining product-kernel models.

### A Product kernels in kernel methods

Product kernels provide a powerful mechanism for constructing high-dimensional similarity measures by combining kernels defined on individual dimensions or feature subsets. This section discusses key examples of product kernels.

**Radial Basis Function (RBF) Kernels as Product Kernels** The RBF kernel is a canonical example of product kernels. The RBF kernel is defined based on a distance metric between two instances, with the two well-known metrics being Euclidean (L2 norm) and Manhattan distances (L1 norm). We refer to the former as RBF, and the latter as Laplacian RBF to distinguish these two kernel functions. In addition, when we have only one kernel bandwidth parameter  $\sigma$ , the RBF kernel is referred to as *isotropic*. The RBF kernel with both distance metrics inherently decomposes into products of univariate kernels across dimensions:

- **RBF Kernel:**

$$K_{\text{RBF}}(\mathbf{x}, \mathbf{z}) = \exp\left(-\frac{\|\mathbf{x} - \mathbf{z}\|^2}{2\sigma^2}\right) = \prod_{i=1}^d \exp\left(-\frac{(x_i - z_i)^2}{2\sigma^2}\right).$$

- **Laplacian RBF Kernel:**

$$K_{\text{Laplacian RBF}}(\mathbf{x}, \mathbf{z}) = \exp\left(-\frac{\|\mathbf{x} - \mathbf{z}\|_1}{\sigma}\right) = \prod_{i=1}^d \exp\left(-\frac{|x_i - z_i|}{\sigma}\right).$$

When alternative distance metrics are incorporated into the RBF kernel, such as the Mahalanobis distance, which involves a covariance matrix, the resulting kernel might lose its product decomposition.

**Automatic Relevance Determination (ARD) in Gaussian Processes** ARD extends RBF kernels by assigning independent length-scale parameters  $\sigma_i$  to each dimension:

$$K_{\text{ARD}}(\mathbf{x}, \mathbf{z}) = \exp\left(-\sum_{i=1}^d \frac{(x_i - z_i)^2}{2\sigma_i^2}\right) = \prod_{i=1}^d \exp\left(-\frac{(x_i - z_i)^2}{2\sigma_i^2}\right).$$

The ARD is extensively used in Gaussian processes for feature selection via learned  $\sigma_i$ , and to enhance interpretability and adaptability. ARD is also referred to as *anisotropic*.

**Cauchy Kernel** The Cauchy kernel, inspired by the Cauchy distribution, is another example of a product kernel:

$$K_{\text{Cauchy}}(\mathbf{x}, \mathbf{z}) = \prod_{i=1}^d \frac{1}{1 + \frac{(x_i - z_i)^2}{\sigma^2}}.$$

**Product of Base Kernels** A popular way for constructing product kernels is by first defining a base kernel for each individual feature and then computing the overall kernel function by multiplying the base kernels over individual features. The product of PSD kernels remains PSD by the Schur product theorem:

$$K(\mathbf{x}, \mathbf{z}) = \prod_{i=1}^d K_i(x_i, z_i).$$

This type of kernel introduces flexibility in combining base kernels while maintaining validity as a (product) kernel function.

## B Newton's identities

To explain Newton's identities, we begin with a specific set of variables  $\mathcal{Z}_4 = \{z_1, z_2, z_3, z_4\}$  before generalising it to sets of arbitrary size  $\mathcal{Z}_d = \{z_1, z_2, \dots, z_d\}$ . The *elementary symmetric polynomials* (ESPs) of degree  $q$  is defined as

$$e_q(\mathcal{Z}_4) = \sum_{1 \leq i_1 < i_2 < \dots < i_q \leq 4} z_{i_1} z_{i_2} \dots z_{i_q},$$

with the conventions  $e_0(\mathcal{Z}_4) = 1$  and  $e_q(\mathcal{Z}_4) = 0$  for  $q > 4$ . For example:

$$\begin{aligned} e_1(\mathcal{Z}_4) &= z_1 + z_2 + z_3 + z_4, \\ e_2(\mathcal{Z}_4) &= z_1 z_2 + z_1 z_3 + z_1 z_4 + z_2 z_3 + z_2 z_4 + z_3 z_4, \\ e_4(\mathcal{Z}_4) &= z_1 z_2 z_3 z_4. \end{aligned}$$

The *power sum* of degree  $r$  is given by

$$p_r(\mathcal{Z}_4) = z_1^r + z_2^r + z_3^r + z_4^r.$$

In particular,  $p_1(\mathcal{Z}_4) = e_1(\mathcal{Z}_4)$  and, for example,  $p_2(\mathcal{Z}_4) = z_1^2 + z_2^2 + z_3^2 + z_4^2$ . Then, Newton's identities relate the ESPs to the power sum recursively. For  $q \geq 1$ ,

$$e_q(\mathcal{Z}_4) = \frac{1}{q} \sum_{r=1}^q (-1)^{r-1} e_{q-r}(\mathcal{Z}_4) p_r(\mathcal{Z}_4).$$

For the set  $\mathcal{Z}_4 = \{z_1, z_2, z_3, z_4\}$ , the identities yield:

$$\begin{aligned} e_1(\mathcal{Z}_4) &= \frac{1}{1} [e_0(\mathcal{Z}_4) p_1(\mathcal{Z}_4)] = p_1(\mathcal{Z}_4) = z_1 + z_2 + z_3 + z_4, \\ e_2(\mathcal{Z}_4) &= \frac{1}{2} [e_1(\mathcal{Z}_4) p_1(\mathcal{Z}_4) - e_0(\mathcal{Z}_4) p_2(\mathcal{Z}_4)] = \frac{(z_1 + z_2 + z_3 + z_4)^2 - (z_1^2 + z_2^2 + z_3^2 + z_4^2)}{2}, \\ e_3(\mathcal{Z}_4) &= \frac{1}{3} [e_2(\mathcal{Z}_4) p_1(\mathcal{Z}_4) - e_1(\mathcal{Z}_4) p_2(\mathcal{Z}_4) + e_0(\mathcal{Z}_4) p_3(\mathcal{Z}_4)], \\ e_4(\mathcal{Z}_4) &= \frac{1}{4} [e_3(\mathcal{Z}_4) p_1(\mathcal{Z}_4) - e_2(\mathcal{Z}_4) p_2(\mathcal{Z}_4) + e_1(\mathcal{Z}_4) p_3(\mathcal{Z}_4) - e_0(\mathcal{Z}_4) p_4(\mathcal{Z}_4)]. \end{aligned}$$

The identities presented above can be extended to sets of arbitrary size  $\mathcal{Z}_d = \{z_1, z_2, \dots, z_d\}$  as

$$e_q(\mathcal{Z}_d) = \frac{1}{q} \sum_{r=1}^q (-1)^{r-1} e_{q-r}(\mathcal{Z}_d) p_r(\mathcal{Z}_d), \quad \text{for } q \geq 1,$$

with  $e_0(\mathcal{Z}_d) = 1$  and  $e_q(\mathcal{Z}_d) = 0$  if  $q > d$  or  $q < 0$ .

## C Proofs

This section provides the detailed proofs of the theoretical results presented in the main paper. First of all, we present a theorem that plays a key role in the other proofs.

**Theorem 10.** *Let the kernel function for feature  $j$  be denoted by  $k_j(x_j, x'_j)$ , and  $\prod_{j \in \emptyset} (k_j(x_j, x'_j) - 1) = 1$  by convention. Then, the following equation holds for product kernel functions:*

$$\prod_{j \in \mathcal{D}} k_j(x_j, x'_j) = \sum_{S \subseteq \mathcal{D}} \prod_{j \in S} (k_j(x_j, x'_j) - 1).$$

**Proof.** We prove the statement by induction on  $|\mathcal{D}|$ .

**Base case** ( $|\mathcal{D}| = 1$ ): Let  $\mathcal{D} = \{j\}$ . Then  $k_j(x_j, x'_j) = 1 + (k_j(x_j, x'_j) - 1)$ , as desired.

**Inductive step:** Assume the equation holds for any set of size  $n$ . Consider a set  $\mathcal{D}$  with size  $n + 1$ , and let  $a \in \mathcal{D}$ . We write:

$$\prod_{j \in \mathcal{D}} k_j(x_j, x'_j) = k_a(x_a, x'_a) \prod_{j \in \mathcal{D} \setminus \{a\}} k_j(x_j, x'_j).$$

Using the induction hypothesis for  $\mathcal{D} \setminus \{a\}$ , we have

$$\prod_{j \in \mathcal{D}} k_j(x_j, x'_j) = k_a(x_a, x'_a) \sum_{\mathcal{T} \subseteq \mathcal{D} \setminus \{a\}} \prod_{j \in \mathcal{T}} (k_j(x_j, x'_j) - 1).$$

Since  $k_a(x_a, x'_a) = (k_a(x_a, x'_a) - 1) + 1$ , expanding gives:

$$\prod_{j \in \mathcal{D}} k_j(x_j, x'_j) = [(k_a(x_a, x'_a) - 1) + 1] \sum_{\mathcal{T} \subseteq \mathcal{D} \setminus \{a\}} \prod_{j \in \mathcal{T}} (k_j(x_j, x'_j) - 1).$$

Expanding this product, we obtain:

$$\prod_{j \in \mathcal{D}} k_j(x_j, x'_j) = \sum_{\mathcal{T} \subseteq \mathcal{D} \setminus \{a\}} (k_a(x_a, x'_a) - 1) \prod_{j \in \mathcal{T}} (k_j(x_j, x'_j) - 1) + \sum_{\mathcal{T} \subseteq \mathcal{D} \setminus \{a\}} \prod_{j \in \mathcal{T}} (k_j(x_j, x'_j) - 1).$$

The first sum on the right-hand side of the equation covers all subsets that contain  $a$ , and the second sum covers all subsets that do not contain  $a$ . Thus, together they sum over all subsets  $S \subseteq \mathcal{D}$ :

$$\prod_{j \in \mathcal{D}} k_j(x_j, x'_j) = \sum_{S \subseteq \mathcal{D}} \prod_{j \in S} (k_j(x_j, x'_j) - 1).$$

Thus, by induction, the theorem is proved.  $\square$

We now provide the proofs for all the theorems and lemmas in the manuscript.

### C.1 Proof of Theorem 1

Using the product kernel and its property in equation (2), the decision function can be rewritten as:

$$f(\mathbf{x}) = \sum_{i=1}^n \alpha_i \prod_{j \in \mathcal{D}} k_j(x_j, x_j^{(i)}).$$

Expanding the product using Theorem 10:

$$\prod_{j \in \mathcal{D}} k_j(x_j, x_j^{(i)}) = \sum_{S \subseteq \mathcal{D}} \prod_{j \in S} (k_j(x_j, x_j^{(i)}) - 1).$$

Substituting this expansion into the decision function:

$$f(\mathbf{x}) = \sum_{i=1}^n \alpha_i \sum_{S \subseteq \mathcal{D}} \prod_{j \in S} (k_j(x_j, x_j^{(i)}) - 1).$$



Rearranging the summations:

$$f(\mathbf{x}) = \sum_{S \subseteq \mathcal{D}} \sum_{i=1}^n \alpha_i \prod_{j \in S} (k_j(x_j, x_j^{(i)}) - 1).$$

This establishes the functional decomposition:

$$f(\mathbf{x}) = \sum_{S \subseteq \mathcal{D}} f_S(\mathbf{x}_S),$$

where each term is uniquely defined as:

$$f_S(\mathbf{x}_S) = \sum_{i=1}^n \alpha_i \prod_{j \in S} (k_j(x_j, x_j^{(i)}) - 1).$$

Since each subset  $S$  contributes independently to the sum and there is no overlap between terms, this decomposition is exact and uniquely determined by the structure of the product kernel.  $\square$

### C.2 Proof of Proposition 3

Based on Definition 2, we have:

$$v_{\mathbf{x}}(S) = \sum_{\mathcal{T} \subseteq S} f_{\mathcal{T}}(\mathbf{x}_{\mathcal{T}}),$$

where  $v_{\mathbf{x}}(S)$  is a unique value function that quantifies the contribution of feature set  $S$  to the prediction. Substituting  $f_{\mathcal{T}}$  from the decomposition, one gets:

$$v_{\mathbf{x}}(S) = \sum_{\mathcal{T} \subseteq S} \sum_{i=1}^n \alpha_i \prod_{j \in \mathcal{T}} (k_j(x_j, x_j^{(i)}) - 1) = \sum_{i=1}^n \alpha_i \sum_{\mathcal{T} \subseteq S} \prod_{j \in \mathcal{T}} (k_j(x_j, x_j^{(i)}) - 1).$$

Using Theorem 10,

$$\sum_{\mathcal{T} \subseteq S} \prod_{j \in \mathcal{T}} (k_j(x_j, x_j^{(i)}) - 1) = \prod_{j \in S} k_j(x_j, x_j^{(i)}),$$

which simplifies the value function to

$$v_{\mathbf{x}}(S) = \sum_{i=1}^n \alpha_i \prod_{j \in S} k_j(x_j, x_j^{(i)}) = \sum_{i=1}^n \alpha_i k_S(\mathbf{x}_S, \mathbf{x}_S^{(i)}),$$

and that completes the proof.  $\square$

### C.3 Proof of Theorem 4

We can write the Shapley value as follows:

$$\phi_j^{\mathbf{x}} := \sum_{S \subseteq \mathcal{D} \setminus \{j\}} \mu(|S|) (v_{\mathbf{x}}(S \cup \{j\}) - v_{\mathbf{x}}(S)) = \sum_{q=0}^{d-1} \mu(q) \sum_{\substack{S \subseteq \mathcal{D} \setminus \{j\} \\ |S|=q}} \left( v_{\mathbf{x}}(S \cup \{j\}) - v_{\mathbf{x}}(S) \right).$$

We now substitute  $v_{\mathbf{x}}(S)$  for the product kernel into the Shapley value formula, one gets:

$$\begin{aligned} \phi_j^{\mathbf{x}} &= \boldsymbol{\alpha}^\top \left( \sum_{q=0}^{d-1} \mu(q) \sum_{\substack{S \subseteq \mathcal{D} \setminus \{j\} \\ |S|=q}} k_{S \cup \{j\}}(\mathbf{X}_{S \cup \{j\}}, \mathbf{x}_{S \cup \{j\}}) - k_S(\mathbf{X}_S, \mathbf{x}_S) \right) \\ &= \boldsymbol{\alpha}^\top \left( \sum_{q=0}^{d-1} \mu(q) \sum_{\substack{S \subseteq \mathcal{D} \setminus \{j\} \\ |S|=q}} k_j(\mathbf{X}_j, x_j) \odot k_S(\mathbf{X}_S, \mathbf{x}_S) - k_S(\mathbf{X}_S, \mathbf{x}_S) \right) \\ &= \boldsymbol{\alpha}^\top \left( \left( k_j(\mathbf{X}_j, x_j) - \mathbf{1} \right) \odot \left( \sum_{q=0}^{d-1} \mu(q) \sum_{\substack{S \subseteq \mathcal{D} \setminus \{j\} \\ |S|=q}} k_S(\mathbf{X}_S, \mathbf{x}_S) \right) \right), \end{aligned} \quad (6)$$

where  $\mathbf{1}$  is a vector of one. Let  $\mathbf{z}_i = k_i(\mathbf{X}_i, x_i)$  and  $\mathcal{Z} = \{\mathbf{z}_1, \dots, \mathbf{z}_d\}$ , one can write:

$$\sum_{\substack{\mathcal{S} \subseteq \mathcal{D} \setminus \{j\} \\ |\mathcal{S}|=q}} k_{\mathcal{S}}(\mathbf{X}, \mathbf{x}) = \sum_{\substack{\mathcal{S} \subseteq \mathcal{D} \setminus \{j\} \\ |\mathcal{S}|=q}} \bigodot_{i \in \mathcal{S}} k_i(\mathbf{X}, \mathbf{x}) = \sum_{\substack{1 \leq i_1 < i_2 < \dots < i_q \leq d-1 \\ j \notin \{i_1, \dots, i_q\}}} \mathbf{z}_{i_1} \odot \mathbf{z}_{i_2} \cdots \odot \mathbf{z}_{i_q} = e_q(\mathcal{Z}_{-j}),$$

where  $e_q(\mathcal{Z}_{-j})$  is the elementary symmetric polynomials. This equation means that the inner sum can be recursively computed by Newton's identities formulation. It then follows:

$$\phi_j^{\mathbf{x}} = \boldsymbol{\alpha}^\top \left( \left( k_j(\mathbf{X}_j, x_j) - \mathbf{1} \right) \bigodot \sum_{q=0}^{d-1} \mu(q) e_q(\mathcal{Z}_{-j}) \right)$$

where

$$e_q(\mathcal{Z}_{-j}) = \frac{1}{q} \sum_{r=1}^q (-1)^{r-1} e_{q-r}(\mathcal{Z}_{-j}) \odot p_r(\mathcal{Z}_{-j}),$$

and  $p_r(\mathcal{Z}) = \sum_{\mathbf{z}_i \in \mathcal{Z}} \mathbf{z}_i^r$  is the power sum, with the power working element-wise. This completes the proof.  $\square$

#### C.4 Proof of Lemma 5

By the efficiency property of Shapley values [1], the sum of Shapley values equals the difference between the value of the grand coalition and the empty coalition:

$$\sum_{j=1}^d \phi_j^{\mathbf{x}} = v_{\mathbf{x}}(\mathcal{D}) - v_{\mathbf{x}}(\emptyset).$$

From Proposition 3, we have:

$$\begin{aligned} v_{\mathbf{x}}(\mathcal{D}) &= \boldsymbol{\alpha}^\top k_{\mathcal{D}}(\mathbf{X}_{\mathcal{D}}, \mathbf{x}_{\mathcal{D}}) = f(\mathbf{x}), \\ v_{\mathbf{x}}(\emptyset) &= \boldsymbol{\alpha}^\top k_{\emptyset}(\mathbf{X}_{\emptyset}, \mathbf{x}_{\emptyset}) = \boldsymbol{\alpha}^\top \mathbf{1} = \sum_{i=1}^n \alpha_i = f_{\emptyset}(\mathbf{x}). \end{aligned}$$

The result follows immediately by substitution.

#### C.5 Proof of Theorem 6

(i) We begin by expressing the full kernel function as a product of feature-wise kernels:

$$k(\mathbf{x}^{(i)}, \mathbf{x}^{(j)}) = \prod_{q \in \mathcal{D}} k_q(x_q^{(i)}, x_q^{(j)}).$$

Using Theorem 10, we expand the product:

$$\prod_{q \in \mathcal{D}} k_q(x_q^{(i)}, x_q^{(j)}) = \sum_{\mathcal{S} \subseteq \mathcal{D}} \prod_{q \in \mathcal{S}} (k_q(x_q^{(i)}, x_q^{(j)}) - 1).$$

Substituting this into the MMD formulation for  $k(\mathbf{x}^{(i)}, \mathbf{x}^{(j)})$ ,  $k(\mathbf{z}^{(i)}, \mathbf{z}^{(j)})$ , and  $k(\mathbf{x}^{(i)}, \mathbf{z}^{(j)})$  yields

$$\begin{aligned} \widehat{\text{MMD}}^2(\mathbb{P}, \mathbb{Q}) &= \frac{1}{n(n-1)} \sum_{i \neq j} \sum_{\mathcal{S} \subseteq \mathcal{D}} \prod_{q \in \mathcal{S}} (k_q(x_q^{(i)}, x_q^{(j)}) - 1) \\ &\quad + \frac{1}{m(m-1)} \sum_{i \neq j} \sum_{\mathcal{S} \subseteq \mathcal{D}} \prod_{q \in \mathcal{S}} (k_q(z_q^{(i)}, z_q^{(j)}) - 1) - \frac{2}{nm} \sum_{i,j} \sum_{\mathcal{S} \subseteq \mathcal{D}} \prod_{q \in \mathcal{S}} (k_q(x_q^{(i)}, z_q^{(j)}) - 1). \end{aligned}$$

By the linearity of summation, we have

$$\begin{aligned} \widehat{\text{MMD}}^2(\mathbb{P}, \mathbb{Q}) &= \sum_{\mathcal{S} \subseteq \mathcal{D}} \left[ \frac{1}{n(n-1)} \sum_{i \neq j} \prod_{q \in \mathcal{S}} (k_q(x_q^{(i)}, x_q^{(j)}) - 1) \right. \\ &\quad \left. + \frac{1}{m(m-1)} \sum_{i \neq j} \prod_{q \in \mathcal{S}} (k_q(z_q^{(i)}, z_q^{(j)}) - 1) - \frac{2}{nm} \sum_{i,j} \prod_{q \in \mathcal{S}} (k_q(x_q^{(i)}, z_q^{(j)}) - 1) \right]. \end{aligned}$$

This establishes the functional decomposition of MMD:

$$\widehat{\text{MMD}}^2(\mathbb{P}, \mathbb{Q}) = \sum_{\mathcal{S} \subseteq \mathcal{D}} f_{\mathcal{S}}^{\text{MMD}}(\mathbb{P}, \mathbb{Q}),$$

where  $f_{\mathcal{S}}^{\text{MMD}}$  is defined as

$$\begin{aligned} f_{\mathcal{S}}^{\text{MMD}}(\mathbb{P}, \mathbb{Q}) &= \frac{1}{n(n-1)} \sum_{i \neq j} \prod_{q \in \mathcal{S}} (k_q(x_q^{(i)}, x_q^{(j)}) - 1) \\ &\quad + \frac{1}{m(m-1)} \sum_{i \neq j} \prod_{q \in \mathcal{S}} (k_q(z_q^{(i)}, z_q^{(j)}) - 1) - \frac{2}{nm} \sum_{i,j} \prod_{q \in \mathcal{S}} (k_q(x_q^{(i)}, z_q^{(j)}) - 1). \end{aligned}$$

- (ii) Following a similar approach as in Proposition 3, we utilize the property that if a function admits a functional decomposition, the corresponding value function for the cooperative game is uniquely defined as:

$$v_{\text{MMD}}(\mathcal{S}) = \sum_{\mathcal{T} \subseteq \mathcal{S}} f_{\mathcal{T}}^{\text{MMD}}(\mathbb{P}, \mathbb{Q}).$$

Applying this to MMD, we define:

$$\begin{aligned} v_{\text{MMD}}(\mathcal{S}) &= \sum_{\mathcal{T} \subseteq \mathcal{S}} \frac{1}{n(n-1)} \sum_{i \neq j} \prod_{q \in \mathcal{T}} (k_q(x_q^{(i)}, x_q^{(j)}) - 1) \\ &\quad + \frac{1}{m(m-1)} \sum_{i \neq j} \prod_{q \in \mathcal{T}} (k_q(z_q^{(i)}, z_q^{(j)}) - 1) - \frac{2}{nm} \sum_{i,j} \prod_{q \in \mathcal{T}} (k_q(x_q^{(i)}, z_q^{(j)}) - 1) \\ &= \frac{1}{n(n-1)} \sum_{i \neq j} \sum_{\mathcal{T} \subseteq \mathcal{S}} \prod_{q \in \mathcal{T}} (k_q(x_q^{(i)}, x_q^{(j)}) - 1) \\ &\quad + \frac{1}{m(m-1)} \sum_{i \neq j} \sum_{\mathcal{T} \subseteq \mathcal{S}} \prod_{q \in \mathcal{T}} (k_q(z_q^{(i)}, z_q^{(j)}) - 1) - \frac{2}{nm} \sum_{i,j} \sum_{\mathcal{T} \subseteq \mathcal{S}} \prod_{q \in \mathcal{T}} (k_q(x_q^{(i)}, z_q^{(j)}) - 1). \end{aligned}$$

By applying Theorem 10 to the inner sum, we can simplify the above equation as:

$$v_{\text{MMD}}(\mathcal{S}) = \frac{1}{n(n-1)} \sum_{i \neq j} k_{\mathcal{S}}(\mathbf{x}_S^{(i)}, \mathbf{x}_S^{(j)}) + \frac{1}{m(m-1)} \sum_{i \neq j} k_{\mathcal{S}}(\mathbf{z}_S^{(i)}, \mathbf{z}_S^{(j)}) - \frac{2}{nm} \sum_{i,j} k_{\mathcal{S}}(\mathbf{x}_S^{(i)}, \mathbf{z}_S^{(j)}),$$

which completes the proof.  $\square$

## C.6 Proof of Proposition 7

By substituting  $v_{\text{MMD}}(\mathcal{S})$  into the Shapley value formula, we obtain:

$$\begin{aligned} \phi_q^{\text{MMD}} &= \sum_{r=0}^{d-1} \mu(r) \sum_{\substack{\mathcal{S} \subseteq \mathcal{D} \setminus \{q\} \\ |\mathcal{S}|=r}} \left( v_{\text{MMD}}(\mathcal{S} \cup \{q\}) - v_{\text{MMD}}(\mathcal{S}) \right) \\ &= \sum_{r=0}^{d-1} \mu(r) \sum_{\substack{\mathcal{S} \subseteq \mathcal{D} \setminus \{q\} \\ |\mathcal{S}|=r}} \left( \frac{1}{n(n-1)} \sum_{i \neq j} (k_q(x_q^{(i)}, x_q^{(j)}) - 1) k_{\mathcal{S}}(\mathbf{x}_S^{(i)}, \mathbf{x}_S^{(j)}) \right. \\ &\quad + \frac{1}{m(m-1)} \sum_{i \neq j} (k_q(z_q^{(i)}, z_q^{(j)}) - 1) k_{\mathcal{S}}(\mathbf{z}_S^{(i)}, \mathbf{z}_S^{(j)}) \\ &\quad \left. - \frac{2}{nm} \sum_{i,j} (k_q(x_q^{(i)}, z_q^{(j)}) - 1) k_{\mathcal{S}}(\mathbf{x}_S^{(i)}, \mathbf{z}_S^{(j)}) \right). \end{aligned}$$

Let  $\mathcal{Z}(\mathbf{x}^{(i)}, \mathbf{x}^{(j)}) = \{k_1(x_1^{(i)}, x_1^{(j)}), \dots, k_d(x_d^{(i)}, x_d^{(j)})\}$  and define the elementary symmetric polynomial as

$$e_r(\mathcal{Z}_{-q}(\mathbf{x}^{(i)}, \mathbf{x}^{(j)})) = \sum_{\substack{\mathcal{S} \subseteq \mathcal{D} \setminus \{q\} \\ |\mathcal{S}|=r}} k_{\mathcal{S}}(\mathbf{x}_S^{(i)}, \mathbf{x}_S^{(j)}).$$

Then, it follows from Newton's identities recurrence:

$$e_r(\mathcal{Z}_{-q}^{(\mathbf{x}^{(i)}, \mathbf{x}^{(j)})}) = \frac{1}{r} \sum_{s=1}^r (-1)^{s-1} e_{r-s}(\mathcal{Z}_{-q}^{(\mathbf{x}^{(i)}, \mathbf{x}^{(j)})}) p_s(\mathcal{Z}_{-q}^{(\mathbf{x}^{(i)}, \mathbf{x}^{(j)})}),$$

where  $p_s(\mathcal{Z}) = \sum_{z \in \mathcal{Z}} z^s$ . Finally, we obtain

$$\begin{aligned} \phi_q^{\text{MMD}} &= \frac{1}{n(n-1)} \sum_{i \neq j} \left( (k_q(x_q^{(i)}, x_q^{(j)}) - 1) \sum_{r=0}^{d-1} \mu(r) e_r(\mathcal{Z}_{-q}^{(x_q^{(i)}, x_q^{(j)})}) \right) \\ &\quad + \frac{1}{m(m-1)} \sum_{i \neq j} \left( (k_q(z_q^{(i)}, z_q^{(j)}) - 1) \sum_{r=0}^{d-1} \mu(r) e_r(\mathcal{Z}_{-q}^{(z_q^{(i)}, z_q^{(j)})}) \right) \\ &\quad - \frac{2}{nm} \sum_{i,j} \left( (k_q(x_q^{(i)}, z_q^{(j)}) - 1) \sum_{r=0}^{d-1} \mu(r) e_r(\mathcal{Z}_{-q}^{(x_q^{(i)}, z_q^{(j)})}) \right), \end{aligned}$$

and that completes the proof.  $\square$

### C.7 Proof of Theorem 8

(i) We begin by expressing the full kernel matrix as a product of feature-wise kernels:

$$\mathbf{K} = \bigodot_{j \in \mathcal{D}} \mathbf{K}_j.$$

since  $\mathbf{K}$  is element-wise products of  $\mathbf{K}_j$ , we can apply Theorem 10 for each element in the kernel matrix and write:

$$\bigodot_{j \in \mathcal{D}} \mathbf{K}_j = \sum_{\mathcal{S} \subseteq \mathcal{D}} \bigodot_{j \in \mathcal{S}} (\mathbf{K}_j - \mathbf{1}\mathbf{1}^\top).$$

Since HSIC is dependent on  $\text{tr}(\mathbf{K}\mathbf{H}\mathbf{L}\mathbf{H})$ , substituting the decomposition of  $\mathbf{K}$  gives:

$$\widehat{\text{HSIC}}(X, y) = \frac{1}{(n-1)^2} \text{tr} \left( \mathbf{H}\mathbf{L}\mathbf{H} \sum_{\mathcal{S} \subseteq \mathcal{D}} \bigodot_{j \in \mathcal{S}} (\mathbf{K}_j - \mathbf{1}\mathbf{1}^\top) \right).$$

Using the linearity of the trace operator, we obtain:

$$\widehat{\text{HSIC}}(X, y) = \frac{1}{(n-1)^2} \sum_{\mathcal{S} \subseteq \mathcal{D}} \text{tr} \left( \mathbf{H}\mathbf{L}\mathbf{H} \bigodot_{j \in \mathcal{S}} (\mathbf{K}_j - \mathbf{1}\mathbf{1}^\top) \right).$$

This completes the proof of the functional decomposition.

(ii) Similar to Proposition 3, we define the value function for a cooperative game as

$$v_{\text{HSIC}}(\mathcal{S}) = \sum_{\mathcal{T} \subseteq \mathcal{S}} \frac{1}{(n-1)^2} \text{tr} \left( \mathbf{H}\mathbf{L}\mathbf{H} \bigodot_{j \in \mathcal{T}} (\mathbf{K}_j - \mathbf{1}\mathbf{1}^\top) \right).$$

By applying Theorem 10, we simplify:

$$\sum_{\mathcal{T} \subseteq \mathcal{S}} \bigodot_{j \in \mathcal{T}} (\mathbf{K}_j - \mathbf{1}\mathbf{1}^\top) = \bigodot_{j \in \mathcal{S}} \mathbf{K}_j.$$

Thus, the value function for feature subset  $\mathcal{S}$  is:

$$v_{\text{HSIC}}(\mathcal{S}) = \frac{1}{(n-1)^2} \text{tr} \left( \mathbf{H}\mathbf{L}\mathbf{H} \bigodot_{j \in \mathcal{S}} \mathbf{K}_j \right) = \frac{1}{(n-1)^2} \text{tr}(\mathbf{H}\mathbf{L}\mathbf{H}\mathbf{K}_{\mathcal{S}}),$$

which completes the proof.  $\square$

### C.8 Proof of Proposition 9

By substituting  $v_{\text{HSIC}}(\mathcal{S}) = \frac{1}{(n-1)^2} \text{tr}(\mathbf{K}_{\mathcal{S}} \mathbf{H} \mathbf{L} \mathbf{H})$  into the Shapley value formula, we obtain:

$$\begin{aligned} \phi_j^{\text{HSIC}} &= \frac{1}{(n-1)^2} \text{tr} \left( \mathbf{H} \mathbf{L} \mathbf{H} \sum_{q=0}^{d-1} \mu(q) \sum_{\substack{\mathcal{S} \subseteq \mathcal{D} \setminus \{j\} \\ |\mathcal{S}|=q}} \left( \mathbf{K}_{\mathcal{S} \cup \{j\}} - \mathbf{K}_{\mathcal{S}} \right) \right) \\ &= \frac{1}{(n-1)^2} \text{tr} \left( \mathbf{H} \mathbf{L} \mathbf{H} \sum_{q=0}^{d-1} \mu(q) \sum_{\substack{\mathcal{S} \subseteq \mathcal{D} \setminus \{j\} \\ |\mathcal{S}|=q}} \left( \mathbf{K}_j \odot \mathbf{K}_{\mathcal{S}} - \mathbf{K}_{\mathcal{S}} \right) \right) \\ &= \frac{1}{(n-1)^2} \text{tr} \left( \mathbf{H} \mathbf{L} \mathbf{H} (\mathbf{K}_j - \mathbf{1} \mathbf{1}^\top) \odot \sum_{q=0}^{d-1} \mu(q) \sum_{\substack{\mathcal{S} \subseteq \mathcal{D} \setminus \{j\} \\ |\mathcal{S}|=q}} \mathbf{K}_{\mathcal{S}} \right). \end{aligned}$$

Letting  $\mathcal{K} = \{\mathbf{K}_1, \dots, \mathbf{K}_d\}$ , we express:

$$\sum_{\substack{\mathcal{S} \subseteq \mathcal{D} \setminus \{j\} \\ |\mathcal{S}|=q}} \mathbf{K}_{\mathcal{S}} = E_q(\mathcal{K}_{-j}),$$

which is computed recursively via Newton's identities formulation:

$$E_q(\mathcal{K}_{-j}) = \frac{1}{d-1} \sum_{r=1}^{d-1} (-1)^{r-1} E_{q-r}(\mathcal{K}_{-j}) \odot P_r(\mathcal{K}_{-j}),$$

where  $P_r(\mathcal{K}) = \sum_{\mathbf{K}_i \in \mathcal{K}} \mathbf{K}_i^r$  is the element-wise power sum polynomial. Substituting this back, we obtain:

$$\phi_j^{\text{HSIC}} = \frac{1}{(n-1)^2} \text{tr} \left( \mathbf{H} \mathbf{L} \mathbf{H} \left( (\mathbf{K}_j - \mathbf{1} \mathbf{1}^\top) \odot \sum_{q=0}^{d-1} \mu(q) E_q(\mathcal{K}_{-j}) \right) \right),$$

which completes the proof.  $\square$

## D Recursive and Numerically Stable Algorithms for Computing Shapley Values for Product-Kernel Learning Models

### D.1 Recursive Algorithm

We present the algorithm for computing the Shapley values for product-kernel learning models. Let  $\mathcal{Z} = \{z_1, \dots, z_d\}$  be a collection of kernel vectors. The elementary symmetric polynomial (ESP) of degree  $q$  is defined as:

$$e_q(\mathcal{Z}) = \sum_{1 \leq i_1 < \dots < i_q \leq d} z_{i_1} \odot \dots \odot z_{i_q}$$

Traditional computation uses Newton's identities:

$$e_q(\mathcal{Z}) = \frac{1}{q} \sum_{k=1}^q (-1)^{k-1} e_{q-k}(\mathcal{Z}) p_k(\mathcal{Z}), \quad p_k(\mathcal{Z}) = \sum_{z_i \in \mathcal{Z}} z_i^k$$

We used this recursion to compute Shapley values in product-kernel learning models. Algorithm 1 summarizes the overall algorithm based on this recursive formulation.

---

**Algorithm 1** Recursive Computaiton of Shapley Values for Product-Kernel Learning Models

---

**Require:** Trained model with product kernels (SVM/SVR/GP), instance  $\mathbf{x} \in \mathbb{R}^d$

**Ensure:** Shapley values  $\phi_1^{\mathbf{x}}, \dots, \phi_d^{\mathbf{x}}$  for each feature

```

1: Retrieve training data  $X$ , coefficients  $\alpha$ , and kernel function  $k$ 
2: Compute feature-wise kernel vectors  $\mathbf{z}_j = k(\mathbf{x}, X), \forall j \in \{1, \dots, d\}$ 
3: Precompute coefficients  $\mu(q) = \frac{q!(d-q-1)!}{d!}, q = 0, \dots, d-1$ 
4: for  $j \in \{1, \dots, d\}$  do
5:   Let  $\mathcal{Z}_{-j} \leftarrow \{\mathbf{z}_1, \dots, \mathbf{z}_d\} \setminus \{\mathbf{z}_j\}$ 
6:   Compute power sums  $p_r(\mathcal{Z}_{-j}) = \sum_{\mathbf{z} \in \mathcal{Z}_{-j}} \mathbf{z}^r$  for  $r = 1, \dots, d-1$ 
7:   Initialize  $e_0 \leftarrow \mathbf{1}$ 
8:   for  $q = 1$  to  $d-1$  do
9:      $e_q(\mathcal{Z}_{-j}) \leftarrow \frac{1}{q} \sum_{r=1}^q (-1)^{k-1} e_{q-r}(\mathcal{Z}_{-j}) \odot p_r(\mathcal{Z}_{-j})$ 
10:  end for
11:   $\psi_j \leftarrow \sum_{q=0}^{d-1} \mu(q) \cdot e_q(\mathcal{Z}_{-j})$ 
12:   $\phi_j^{\mathbf{x}} \leftarrow \alpha^\top ((\mathbf{z}_j - \mathbf{1}) \odot \psi_j)$ 
13: end for
14:
15: return  $(\phi_1^{\mathbf{x}}, \dots, \phi_d^{\mathbf{x}})$ 

```

---

Though being efficient, the recursive formulation suffers from numerical instability due to alternating sign cancellation, power operations, and error amplification through division. To develop a stable approach, we use the fact that symmetric elementary polynomials emerge naturally as coefficients of the characteristic polynomial [34]:

$$P(\mathbf{x}) = \bigodot_{i=1}^d (\mathbf{x} - \mathbf{z}_i) = \sum_{q=0}^d (-1)^{d-q} e_{d-q}(\mathcal{Z}) \mathbf{x}^q.$$

Initialize  $P_0(\mathbf{x}) = \mathbf{1}$ . For each  $\mathbf{z}_i$ , the update rule is

$$P_i(\mathbf{x}) = P_{i-1}(\mathbf{x}) \odot (\mathbf{x} - \mathbf{z}_i),$$

and the coefficients evolve as

$$\text{Coeff}_m^{(i)} = \text{Coeff}_{m-1}^{(i-1)} - \left( \mathbf{z}_i \odot \text{Coeff}_m^{(i-1)} \right),$$

where  $\text{Coeff}_m^{(i)}$  denotes the coefficient of  $\mathbf{x}^m$  after processing  $i$  elements. The elementary symmetric polynomials are then:

$$e_q(\mathcal{Z}) = (-1)^{d-q} \cdot \text{Coeff}_q^{(d)}.$$

Using this relationship, we can avoid the power and division operations in the standard recursive formulation and develop a more stable algorithm to compute ESPs. Aside from this, we scale kernel vectors  $\mathbf{z}_i \leftarrow \mathbf{z}_i/s$  where  $s = \max_{i,j} z_{ij}$  to prevent overflow, with final correction  $e_q \leftarrow e_q \cdot s^q$ . Algorithm 2 shows the numerically stable algorithm for computing Shapley values for product-kernel learning models. This algorithm has the same complexity as Algorithm 1, but it avoids the power and division, which makes it more numerically stable (especially for high values of  $d$ ).

## E Additivity of Explanations for Learning Models, MMD and HSIC

### E.1 Explanation Additivity for Learning Models

In Lemma 5, we established the additivity property of the explanation in product-kernel learning models. In particular, we demonstrated that

$$f(\mathbf{x}) - \alpha^\top \mathbf{1} = \sum_j \phi_j^{\mathbf{x}},$$

---

**Algorithm 2** Numerically Stable Shapley Values Computation

---

**Require:** Trained model with product kernels (SVM/SVR/GP), instance  $\mathbf{x} \in \mathbb{R}^d$

**Ensure:** Shapley values  $\phi_1^{\mathbf{x}}, \dots, \phi_d^{\mathbf{x}}$  for each feature

```

1: Retrieve training data  $X$ , coefficients  $\alpha$ , and kernel function  $k$ 
2: Compute feature-wise kernel vectors  $\mathbf{z}_j = k(\mathbf{x}, X), \forall j \in \{1, \dots, d\}$ 
3: Precompute coefficients  $\mu(q) = \frac{q!(d-q-1)!}{d!}, q = 0, \dots, d-1$ 
4: for  $j = 1$  to  $d$  do
5:    $\mathcal{Z}_{-j} \leftarrow \{\mathbf{z}_1, \dots, \mathbf{z}_d\} \setminus \{\mathbf{z}_j\}$ 
6:   Scale  $\mathcal{Z}_{-j}$ :  $s \leftarrow \max_{i,j} \mathbf{z}_{ij} \forall \mathbf{z}_i \in \mathcal{Z}_{-j}$  (or 1 if all 0)
7:    $\tilde{\mathcal{Z}}_{-j} \leftarrow \{\mathbf{z}_i/s \mid \mathbf{z}_i \in \mathcal{Z}_{-j}\}$ 
8:   Coeff  $\leftarrow [1] \{P_0(\mathbf{x}) = 1\}$ 
9:   for  $\tilde{\mathbf{z}}_i \in \tilde{\mathcal{Z}}_{-j}$  do
10:    new_coeff  $\leftarrow []$ 
11:    Append  $-\tilde{\mathbf{z}}_i \cdot \text{Coeff}[0]$  to new_coeff {Term for  $\mathbf{x}^0$ }
12:    for  $k = 1$  to  $\text{len}(\text{Coeff}) - 1$  do
13:      term  $\leftarrow \text{Coeff}[k-1] - (\tilde{\mathbf{z}}_i \odot \text{Coeff}[k])$ 
14:      Append term to new_coeff
15:    end for
16:    Append Coeff[-1] to new_coeff
17:    Coeff  $\leftarrow$  new_coeff
18:  end for
19:  Extract  $e_q(\mathcal{Z}_{-j})$ :  $e_q(\mathcal{Z}_{-j}) \leftarrow (-1)^q \cdot \text{Coeff}[d-q-1] \cdot s^q$  for  $q = 0, \dots, d-1$ 
20:   $\psi_j \leftarrow \sum_{q=0}^{d-1} \mu(q) \odot e_q(\mathcal{Z}_{-j})$ 
21:   $\phi_j^{\mathbf{x}} \leftarrow \alpha^\top ((\mathbf{z}_j - \mathbf{1}) \odot \psi_j)$ 
22: end for
23: return  $(\phi_1^{\mathbf{x}}, \dots, \phi_d^{\mathbf{x}})$ 

```

---

where  $\alpha^\top \mathbf{1}$  represents the value of the null game according to the value function in (4). This result is useful since  $\alpha^\top \mathbf{1} = 0$  for several kernel methods such as support vector machines (we have the constraint  $\sum \hat{\alpha}_j y_j = 0$  in the dual problem and  $f(\mathbf{x}) = \sum_j \hat{\alpha}_j y_j k(\mathbf{x}, \mathbf{x}_j)$  with  $\hat{\alpha}$  be the solution to the dual problem) and support vector regression. However, in general, it distributes the value of  $f(\mathbf{x})$  only after subtracting the null game's value rather than allocating the full output  $f(\mathbf{x})$  directly among the features. This is because  $k_\emptyset = 1$  by definition, and this will lead to  $v(\emptyset) = \alpha^\top \mathbf{1}$ . We now show that by redefining the value function in (4) so that  $v(\emptyset) = 0$ , the corresponding Shapley values will sum to  $f(\mathbf{x})$ , with each Shapley value augmented by  $\frac{\alpha^\top \mathbf{1}}{n}$ .

**Proposition 11.** *Define a normalized value function by setting the kernel component for the empty set to zero, i.e.,  $k_\emptyset = 0$ . Let  $\hat{v}_{\mathbf{x}}$  be the corresponding value function and  $\hat{\phi}_j$  the resulting Shapley values, which satisfy*

$$f(\mathbf{x}) = \sum_{j=1}^n \hat{\phi}_j.$$

*Then, assuming an equal allocation of the baseline value, the following relationship holds for every feature  $j$ :*

$$\hat{\phi}_j = \phi_j + \frac{\alpha^\top \mathbf{1}}{n}.$$

**Proof** Using the efficiency axioms for  $\hat{v}_{\mathbf{x}}$ , the results will follow.

## E.2 Explanation Additivity for MMD

**Lemma 12.** *For the MMD with product kernel, the sum of Shapley values satisfies:*

$$\sum_{j=1}^d \phi_j^{\text{MMD}} = \widehat{\text{MMD}}^2(\mathbb{P}, \mathbb{Q}).$$

**Proof** By the efficiency property of Shapley values [1]:

$$\sum_{j=1}^d \phi_j^{\text{MMD}} = v_{\text{MMD}}(\mathcal{D}) - v_{\text{MMD}}(\emptyset)$$

For the product-kernel decomposition:

$$v_{\text{MMD}}(\mathcal{D}) = \frac{1}{n(n-1)} \sum_{i \neq j} k(\mathbf{x}^{(i)}, \mathbf{x}^{(j)}) + \frac{1}{m(m-1)} \sum_{i \neq j} k(\mathbf{y}^{(i)}, \mathbf{y}^{(j)}) - \frac{2}{nm} \sum_{i,j} k(\mathbf{x}^{(i)}, \mathbf{y}^{(j)}) = \widehat{\text{MMD}}^2(\mathbb{P}, \mathbb{Q})$$

For the empty coalition (all features removed):

$$v_{\text{MMD}}(\emptyset) = \frac{1}{n(n-1)} \sum_{i \neq j} 1 + \frac{1}{m(m-1)} \sum_{i \neq j} 1 - \frac{2}{nm} \sum_{i,j} 1 = \frac{n(n-1)}{n(n-1)} + \frac{m(m-1)}{m(m-1)} - \frac{2nm}{nm} = 0$$

$$\text{Thus, } \sum_{j=1}^d \phi_j^{\text{MMD}} = \widehat{\text{MMD}}^2(\mathbb{P}, \mathbb{Q}) - 0 = \widehat{\text{MMD}}^2(\mathbb{P}, \mathbb{Q}). \quad \square$$

### E.3 Explanation Additivity for HSIC

**Lemma 13.** *For the HSIC dependence measure with a product kernel, the sum of Shapley values satisfies:*

$$\sum_{j=1}^d \phi_j^{\text{HSIC}} = \widehat{\text{HSIC}}(X, y).$$

**Proof** By the efficiency property of Shapley values [1], the sum of Shapley values equals the difference between the value of the grand coalition and the empty coalition:

$$\sum_{j=1}^d \phi_j^{\text{HSIC}} = v_{\text{HSIC}}(\mathcal{D}) - v_{\text{HSIC}}(\emptyset).$$

From Theorem 8 (ii), we have:

$$v_{\text{HSIC}}(\mathcal{D}) = \frac{1}{(n-1)^2} \text{tr} \left( \mathbf{H} \mathbf{L} \mathbf{H} \bigodot_{j \in \mathcal{D}} \mathbf{K}_j \right) = \widehat{\text{HSIC}}(X, y),$$

$$v_{\text{HSIC}}(\emptyset) = \frac{1}{(n-1)^2} \text{tr}(\mathbf{H} \mathbf{L} \mathbf{H} \mathbf{1} \mathbf{1}^\top).$$

One can simply realize that  $\mathbf{H} \mathbf{L} \mathbf{H} \mathbf{1} \mathbf{1}^\top = 0$  as the sum of rows and columns in  $H$  is zero, and substituting these into the efficiency property completes the proof.  $\square$

## F HSIC attribution with two multivariate variables

We studied the Shapley value computation for HSIC when it measures dependence between a multivariate variable  $\mathbf{x}$  and a univariate target  $y$ . We now extend this framework to two multivariate variables  $X \in \mathbb{R}^d$  and  $Z \in \mathbb{R}^d$  with product kernels function  $k$  and  $l$ . Given a sample  $\{(\mathbf{x}^{(i)}, \mathbf{z}^{(i)})\}_{i=1}^n \sim \mathbb{P}(X, Z)$ ,  $\text{HSIC}(X, Z)$  can be estimated as:

$$\widehat{\text{HSIC}}(X, Z) = \frac{1}{(n-1)^2} \text{tr}(\mathbf{H} \mathbf{K} \mathbf{H} \mathbf{L}),$$

where  $\mathbf{K} \in \mathbb{R}^{n \times n}$  is the kernel matrix computed using the kernel  $k$ , i.e.  $\mathbf{K}_{ij} = k(\mathbf{x}^{(i)}, \mathbf{x}^{(j)})$ ,  $\mathbf{L} \in \mathbb{R}^{n \times n}$  is the kernel matrix computed using the kernel  $l$ , i.e.  $\mathbf{L}_{ij} = l(\mathbf{z}^{(i)}, \mathbf{z}^{(j)})$ , and  $\mathbf{H} = I - \frac{1}{n} \mathbf{1} \mathbf{1}^\top$  is the centering matrix ensuring zero mean in the feature space.

To address the attribution to variables in both  $X$  and  $Z$ , we establish two cooperative games to attribute dependence contributions: For product kernels  $k$  and  $l$ , we define two value functions for the two games:



- (i) We first assume that  $\mathbf{L}$  is fixed, and try to attribute the total HSIC to the variables in  $X$ . Since  $k$  is a product kernel, we can recover a functional decomposition based on  $k$ , similar to Theorem 8. Let  $\mathcal{D}_X$  be the set of variables of  $X$ , we therefore define the value function for attributing the total HSIC to  $X$  variables as:

$$v_{\text{HSIC}_X}(\mathcal{S}) = \frac{1}{(n-1)^2} \text{tr}(\mathbf{H}\mathbf{K}_{\mathcal{S}}\mathbf{H}\mathbf{L}), \quad \forall \mathcal{S} \subseteq \mathcal{D}_X. \quad (7)$$

- (ii) By the same token, we take  $\mathbf{K}$  fixed and try to attribute the total HSIC to the variables in  $Z$ . Since  $l$  is a product kernel, we can recover a functional decomposition based on  $l$  and define the value function as:

$$v_{\text{HSIC}_Z}(\mathcal{S}) = \frac{1}{(n-1)^2} \text{tr}(\mathbf{H}\mathbf{K}\mathbf{H}\mathbf{L}_{\mathcal{S}}), \quad \forall \mathcal{S} \subseteq \mathcal{D}_Z, \quad (8)$$

where  $\mathcal{D}_Z$  is the set of variables of  $Z$ .

Building on the two value functions, we can compute Shapley values for variables in  $X$  and  $Z$  separately. We denote the Shapley value of variable  $j$  for  $X$  and  $Z$  as  $\phi_j^{\text{HSIC}_X}$  and  $\phi_j^{\text{HSIC}_Z}$ , respectively. These values are interpreted as:

- $\phi_j^{\text{HSIC}_X}$  quantifies the contribution of the  $j^{\text{th}}$  variable in  $X$  to the total dependence between  $X$  and  $Z$ ;
- $\phi_j^{\text{HSIC}_Z}$  quantifies the contribution of the  $j^{\text{th}}$  variable in  $Z$  to the total dependence between  $X$  and  $Z$ .

## G Experiments

### G.1 Experimental Setup

**SVM Optimization Using Optuna [45]** When using SVM in our experiments, we optimized the Support Vector Machine (SVM) with a Radial Basis Function (RBF) kernel using Optuna [45], a robust hyperparameter optimization framework. The target type (either 'regression' or 'classification') was determined to guide the selection of the appropriate SVM model (SVR for regression and SVC for classification). The hyperparameters  $C$  and  $\gamma$ , critical for the RBF kernel's performance, were optimized within an extensive range using a log-uniform distribution. Specifically, we defined the hyperparameters:  $C$  between  $10^{-5}$  and  $10^5$  and  $\gamma$  between  $10^{-5}$  and  $10^3$ , and utilized 5-fold cross-validation to ensure reliable evaluation. The optimization process aimed to minimize the mean squared error for regression tasks and maximize accuracy for classification tasks. After conducting the specified number of trials ( $n=100$ ), the best hyperparameters were used to train a final SVM model on the entire dataset, yielding both the optimal model configuration and the best cross-validation score achieved during the optimization process.

**Training Gaussian Process (GP) Using K-Fold Cross-Validation** When using GP, we trained a model using k-fold cross-validation to ensure robust evaluation and generalization performance. We defined the GP kernel as  $\mathcal{C}(1.0, (1e-4, 1e1)) * \text{RBF}(1.0, (1e-4, 10))$ , suitable for both regression and classification tasks. For classification problems, `GaussianProcessClassifier` was utilized, while `GaussianProcessRegressor` was used for regression tasks. We employed K-Fold with  $K = 5$  for cross-validation to evaluate the model's performance across different folds. All the hyperparameters, including the kernel width of the RBF kernel, are determined in the training process using optimization. During the cross-validation process, the model was trained on each fold, and predictions were made on the validation fold. Performance metrics were chosen based on the problem type: accuracy for classification models and mean absolute percentage error (MAPE) for regression models. The scores from each fold were aggregated to compute the average and standard deviation of the scores.

### G.2 MMD Experiments

In addition to the synthetic experiments for MMD, we first provide another experiment for the cases when there is no distribution discrepancy. To that end,  $X$  and  $Z$  are sampled from the same

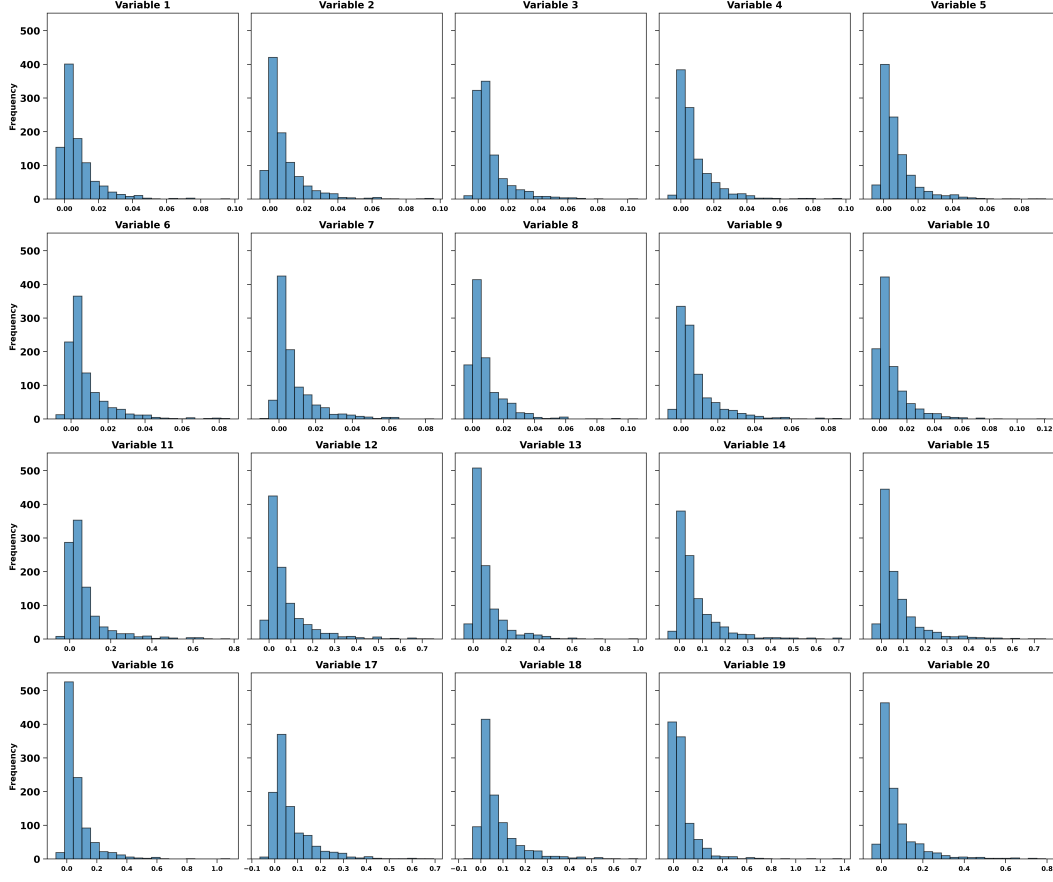


Figure 5: Shapley values for the synthetic data sets with equal distributions. All variables contribute equally to the near-zero MMD.

multivariate normal distribution across all 20 variables. The MMD is near zero, indicating the distributions are equivalent. Shapley values are computed and replicated 1000 times, with histograms plotted for each variable in Figure 5. The near-identical distributions of Shapley values across all variables reflect the uniform contribution of these variables to the MMD close to zero, consistent with the absence of any significant difference between the distributions.

We extend our analysis to the UCI Diabetes dataset, consisting of 442 samples and 10 baseline variables, including age, sex, body mass index (BMI), average blood pressure, and six blood serum measurements (shown by  $s1$  to  $s6$  features). The dataset is split into male and female subsets using the second variable (sex), which is excluded from the analysis, leaving nine variables for comparison.

Using MMD, we calculate the dissimilarity between male and female groups and then compute Shapley values to attribute variable contributions to the MMD. Figure 6 displays the Shapley values for the nine variables in the Diabetes dataset. The results show that  $s3$  and  $s4$  contribute most significantly to the MMD, followed by  $bp$ ,  $s6$ ,  $age$ ,  $s5$ , and  $s2$ . In contrast,  $bmi$  and  $s1$  reduce the MMD, indicating their alignment across the two groups.

To validate these results, we analyze the marginal distributions of variables for males and females, as shown in Figure 7. The analysis confirms that variables with distinct marginal distributions between males and females (e.g.,  $s3$  and  $s4$ ) have high positive Shapley values, reflecting their role in increasing the MMD. Conversely, variables with similar distributions (e.g.,  $s1$ ) exhibit negative Shapley values, highlighting their role in reducing the MMD.

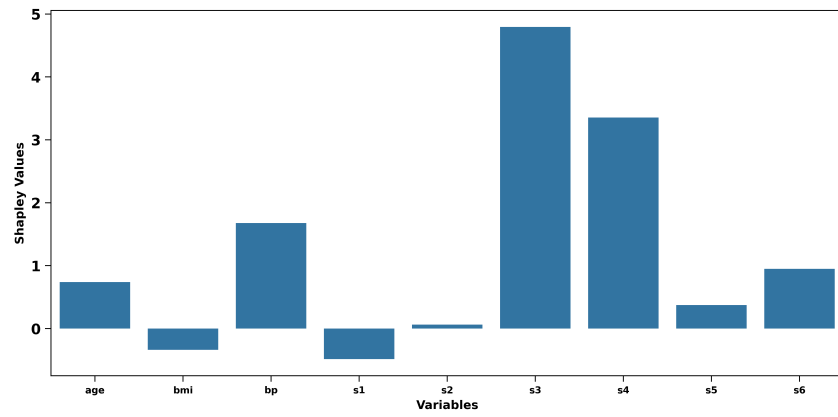


Figure 6: Shapley values explaining MMD between male and female subsets in the UCI Diabetes data set.

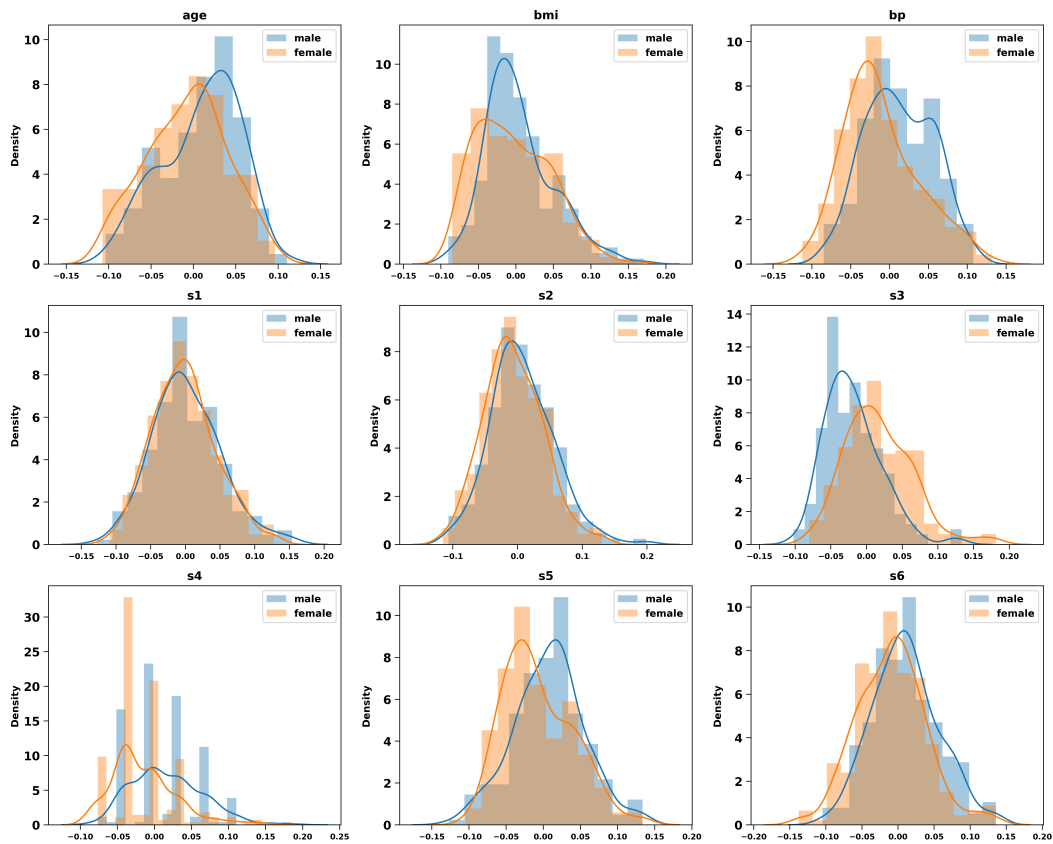


Figure 7: Marginal distributions of variables for male and female subsets in the UCI Diabetes dataset.